https://doi.org/10.1093/plphys/kiac489 PLANT PHYSIOLOGY 2023: 191: 660–678

Plant Physiology®

Research Article

A conserved protein disulfide isomerase enhances plant resistance against herbivores

Jia-Rong Cui ,[1] Xiao-Li Bing ,[1,*] Yi-Jing Tang,[1] Fan Liu,[1] Lu Ren,[1] Jia-Yi Zhou,[1] Huan-Huan Liu ,[1] Meng-Ke Wang,[1] Ary A. Hoffmann[2] and Xiao-Yue Hong [1,*]

1 College of Plant Protection, Nanjing Agricultural University, Nanjing, Jiangsu 210095, China
2 School of BioSciences, Bio21 Institute, The University of Melbourne, Parkville, VIC 3010, Australia

*Author for correspondence: xyhong@njau.edu.cn (X.-Y.H.), xlbing@njau.edu.cn (X.-L.B.)
These authors contributed equally (J.-R.C. and X.-L.B.).
X.-Y.H., X.-L.B., and J.-R.C. designed the research; J.-R.C., X.-L.B., Y.-J.T., F.L., L.R., and J.-Y.Z., performed the research; J.-R.C., X.-L.B., A. A.H., and H.-H.L. analyzed the data; J.-R.C., X.-L.B., A. A.H., and X.-Y.H. wrote the paper.
The authors responsible for distribution of materials integral to the findings presented in this article in accordance with the policy described in the Instructions for Authors (https://academic.oup.com/plphys/pages/general-instructions) are: Xiao-Yue Hong (xyhong@njau.edu.cn), Xiao-Li Bing (xlbing@njau.edu.cn).

Abstract

Herbivore-associated molecular patterns (HAMPs) enable plants to recognize herbivores and may help plants adjust their defense responses. Here, we report on herbivore-induced changes in a protein disulfide isomerase (PDI) widely distributed across arthropods. PDI from the spider mite *Tetranychus evansi* (TePDI), a mesophyll-feeding agricultural pest worldwide, triggered immunity in multiple Solanaceae plants. TePDI-mediated cell death in *Nicotiana benthamiana* required the plant signaling proteins SGT1 (suppressor of the G2 allele of skp1) and HSP90 (heat shock protein 90), but was suppressed by spider mite effectors Te28 and Te84. Moreover, PDIs from phylogenetically distinct herbivorous and nonherbivorous arthropods triggered plant immunity. Finally, although PDI-induced plant defenses impaired the performance of spider mites on plants, RNAi experiments revealed that *PDI* genes are essential for the survival of mites and whiteflies. Our findings indicate that plants recognize evolutionarily conserved HAMPs to activate plant defense and resist pest damage, pointing to opportunities for broad-spectrum pest management.

Introduction

Plants and herbivores are engaged in a constant arms race. Piercing–sucking herbivores such as planthoppers, whiteflies, and spider mites secrete salivary compounds when inserting their stylets into phloem or mesophyll cells (van Bell and Will, 2016), including effector proteins to suppress plant defenses (Hogenhout and Bos, 2011). Many salivary effectors that help suppress plant defenses have been identified, such as MpC002 from aphids (Bos et al., 2010), Bt56 from whiteflies (Xu et al., 2019), DNase II and Vg from rice planthoppers (Huang et al., 2019b; Ji et al., 2021), and Te28 and Te84 from spider mites (Villarroel et al., 2016). Meanwhile, herbivore saliva also contains many "elicitors" that induce plant defense responses (Erb and Reymond, 2019). These elicitors are collectively called herbivore-associated molecular patterns (HAMPs; Snoeck et al., 2022). The first reported HAMP, β-glucosidase, was isolated from the regurgitant of the large white butterfly (*Pieris brassicae*; Mattiacci et al., 1995), while HAMPs from Hemipteran pests include mucin-like protein (NIMLP) from the brown planthopper (*Nilaparvata lugens*; Shangguan et al., 2018) and CathB3 from the green peach aphid (*Myzus persicae*; Guo et al.,

Received July 05, 2022. Accepted October 05, 2022. Advance access publication October 21, 2022
© American Society of Plant Biologists 2022. All rights reserved. For permissions, please email: journals.permissions@oup.com

2020). Some HAMPs are relatively conserved in their ability to induce responses across a range of plant species, such as Nl16 and Nl32 in planthoppers (Rao et al., 2019), MP10 in aphids (Bos et al., 2010), and GOX in caterpillar species (Musser et al., 2002). Until now, only two mite-specific elicitors (called "tetranins" Tet1 and Tet2) from the spider mite *Tetranychus urticae* have been reported to induce plant defenses (Iida et al., 2019), but conserved HAMPs have not been identified from this pest group.

Plants have evolved a complex immune system to fend off attacks from herbivores as well as pathogens. Cell membrane- embedded pattern recognition receptors (PRRs) can recognize pathogen-associated molecular patterns (PAMPs) as well as HAMPs. The recognition of PAMPs results in PAMP-triggered immunity (PTI; Monaghan and Zipfel, 2012; Schwessinger and Ronald, 2012). Co-receptors BAK1 (BRI1-associated kinase1) and SOBIR1 (suppressor of BIR1-1) are the major modulators of PTI signaling. There is growing evidence that many PAMPs, such as XEG1 (Ma et al., 2015) and VmE02 (Nie et al., 2019), require BAK1 to trigger immune signaling. PRRs also occupy a fundamental role in herbivore resistance in plants. The *Arabidopsis bak1* mutant, for instance, decreases resistance to aphids because of reduced reactive oxygen species (ROS) accumulation and callose deposition (Prince et al., 2014). Apart from PTI, plants develop nucleotide-binding leucine-rich repeat (NLR) receptors to specifically recognize effectors in the cytoplasm, ultimately resulting in effector-triggered immunity (ETI; Jones and Dangl, 2006; Jones et al., 2016). Modulators of ETI signaling include SGT1, HSP90, and RAR1 (required for Mla12 Resistance 1) that mediate the stability of NLR proteins (Mayor et al., 2007). In addition, nonrace-specific disease resistance 1 (NDR1) and enhanced disease susceptibility1 (EDS1) are involved in NLR protein-mediated signaling (Chen et al., 2021). These ETI-related signaling molecules participate in plant–herbivore interactions. For example, SGT1 and HSP90 are required for *Mi-1* in mediating resistance of tomato (*Solanum lycopersicum*) plants against aphids and whiteflies (Bhattarai et al., 2007). SGT1 also regulates *Nicotiana attenuata*'s resistance to the chewing herbivore *Manduca sexta* (Meldau et al., 2011). EDS1, an essential component of the SA pathway, is necessary for the induction of defense genes in response to the oviposition of *P. brassicae* (Gouhier-Darimont et al., 2013). However, information on the mechanisms involved in HAMP-induced immune response by plants remains limited.

The tomato red spider mite, *Tetranychus evansi* Baker and Pritchard, is a worldwide pest of *Solanaceous* crops and causes enormous economic damage in many regions of the world (Navajas et al., 2013). *Tetranychus evansi* is a cell-content feeder that feeds on mesophyll cells with cheliceral stylets (Alba et al., 2015). During feeding, *T. evansi* suppresses defense in tomato plants by suppressing the downstream expression of the SA pathway, JA pathway, and proteinase inhibitors (Sarmento et al., 2011; Alba et al., 2015; Schimmel et al., 2018). *Tetranychus evansi* contains effector proteins, such as Te28 and Te84, that suppress defenses and thereby enhance mites performance on *Nicotiana benthamiana* (Villarroel et al., 2016). However, whether *T. evansi* has HAMPs that activate plant defenses remains unknown. Here, we build on previous work on the identification of salivary proteins from *T. evansi* (Huang et al., 2019a) to identify one protein, disulfide isomerase (PDI, most likely from mite saliva), that acts as a HAMP and that is involved in plant–arthropod interactions.

PDI is a multifunctional enzyme that acts as both a thiol-disulfide oxidoreductase and a molecular chaperone in many organisms (Khan and Mutus, 2014). The typical PDI protein contains a signal peptide, two thioredoxin-like catalytic domains (a and a′), two noncatalytic domains (b and b′), two active site motifs (CGHC), and endoplasmic reticulum (ER) retention signal (Narindrasorasak et al., 2003). PDIs have been identified in pathogens (Meng et al., 2015), nematodes (Zhao et al., 2020), insects (Fu et al., 2021), and mites (Zhu et al., 2018). Secreted PDIs of pathogens and nematodes function as a virulence factor during host infection, but also induce plant immune responses. For instance, the PDI from *Phytophthora parasitica* (PpPDI1) induces cell death in *N. benthamiana* but enhances pathogen virulence during infection (Meng et al., 2015). MiPDI1 from the root-knot nematode *Meloidogyne incognita*, protects nematodes from oxidative stress (Zhao et al., 2020). In the small brown planthopper, *Laodelphax striatellus*, a secreted PDI (LsPDI1) activates plant immunity responses and contributes to plant resistance against pests (Fu et al., 2021). However, how PDI triggers plant immunity and the universality of PDI-triggered immunity across arthropods remain unclear.

In this study, we found that TePDI, a HAMP from *T. evansi*, triggers plant defenses by inducing ROS burst, callose deposition, and plant defense-related changes in gene expression. We show that TePDI induces defenses across different plant species. We identify plant signaling components and functional domains responsible for TePDI-induced cell death, and we undertake an evolutionary analysis to show that PDI proteins are conserved across arthropods and are subject to purifying selection. We also demonstrate that PDIs in nonherbivorous insects can activate plant defenses, suggesting functional conservation of PDI proteins.

Results

Infestation of *T. evansi* activates defense responses in *N. benthamiana*

To explore the interaction between *T. evansi* and plants, we measured multiple indicators of plant defense after infestation of *N. benthamiana* by spider mites. Our results showed that *T. evansi* infestation induced cell death (Figure 1A). Compared with the uninfested controls, *T. evansi*-infested leaves showed ROS accumulation (Figure 1B) and more callose deposition (Figure 1, C and D). In addition, the expression levels of SA (salicylic acid)-related genes *NPR1* (nonexpressor of pathogenesis-related genes1) and *PR1a* (pathogenesis-related protein 1a), and JA-related genes *PR3*

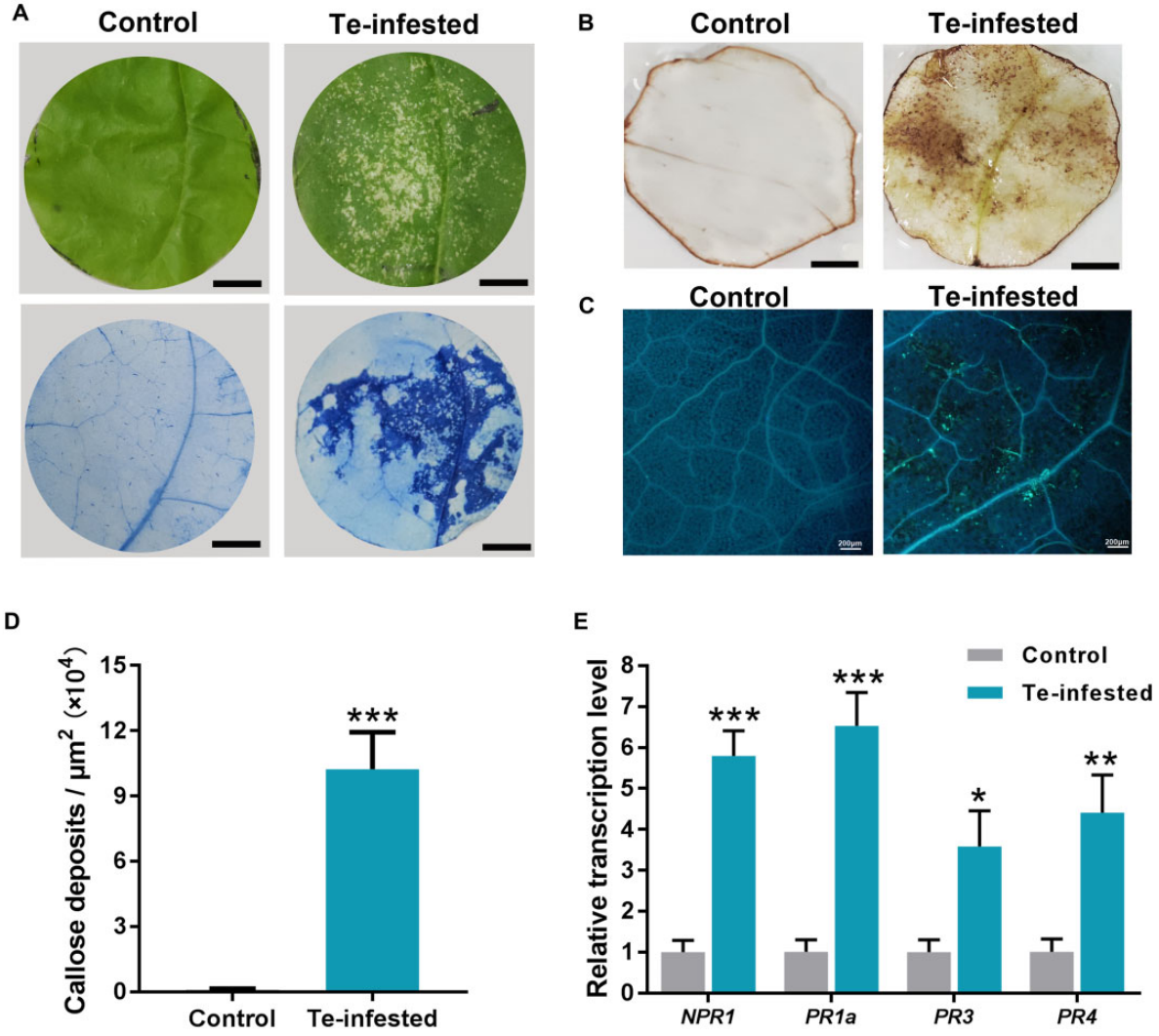

Figure 1 *Tetranychus evansi* infestation induces cell death and defense responses. A, Infestation of *T. evansi* induced cell death in *N. benthamiana*. Te-infested indicates *N. benthamiana* leaves that were infested by 30 *T. evansi* adults for 24 h and were stained with Trypan Blue. The control treatment represents uninfested tobacco leaves. Scale bar = 50 mm. B, ROS accumulation in *T. evansi*-infested leaves and control leaves. Scale bar = 50 mm. C and D, Callose deposition in *N. benthamiana* (C) and the area of callose spots on leaf discs (D). Scale bar = 200 μm. $n = 6$. E, Relative expression of plant defense-related marker genes in *N. benthamiana* leaves. Leaves were collected at 24 h after infestation by 30 *T. evansi* mites. Relative gene expression was normalized to *Nbrpl23* and calibrated to the levels of the controls (set as 1). $n = 3$. Asterisks represent statistically significant differences based on Student's *t* test (*$P < 0.05$, **$P < 0.01$, ***$P < 0.001$); error bars represent SEM.

(pathogenesis-related protein 3) and *PR4* (pathogenesis-related protein 4) were significantly upregulated in leaves infested by *T. evansi* relative to control leaves (Figure 1E). These results indicated that *T. evansi* triggered plant defense responses when feeding on *N. benthamiana*.

TePDI from *T. evansi* induces plant defense responses

To identify key proteins that induce plant defense responses, we screened the previously discovered 136 *T. evansi* salivary proteins (Huang et al., 2019a). As is shown in the workflow (Supplemental Figure S1A), we first considered 61 salivary proteins containing signal peptides. Among these, 11 proteins with transmembrane domains were removed. After removing the redundant proteins, we finally selected 23 proteins from this group and cloned the coding sequences (CDS) of each gene, inserted them into expression vectors of *Agrobacterium tumefaciens*, and transiently expressed them in *N. benthamiana* leaves to test if cell death occurs. Among the 23 candidates (Supplemental Table S1), Te16 and Te21 induced cell death in *N. benthamiana* leaves (Supplemental Figure S1B). In addition, *T. evansi* expressed significantly more *Te21* after feeding on *N. benthamiana* (Supplemental Figure S1D), which highlighted the importance of Te21 in mite–plant interactions. InterPro annotation results showed that Te21 is a protein disulfide isomerase (abbreviated as PDI), so we referred to Te21 as TePDI.

Knowing that TePDI can induce cell death in *N. benthamiana* (Figure 2A), we further explored the plant defense-

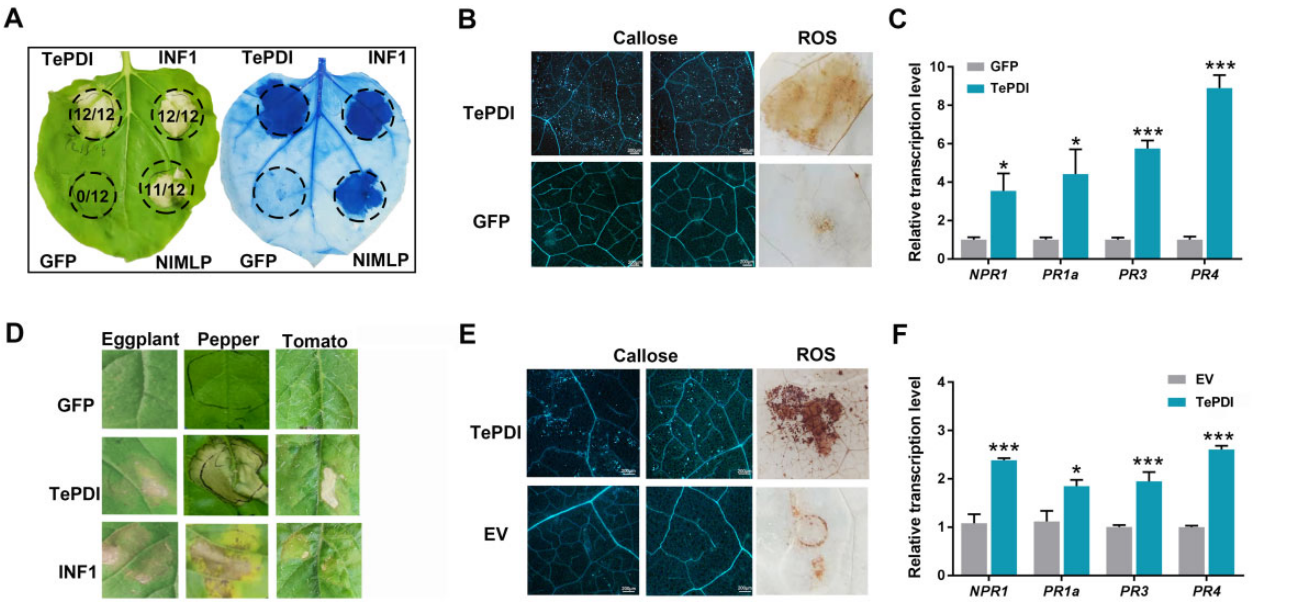

Figure 2 TePDI is an elicitor that induces defense responses. A, TePDI-induced cell death in *N. benthamiana*. Transient expression of *TePDI*, *GFP*, *INF1*, and *NIMLP* in *N. benthamiana*. GFP was used as the negative control, INF1 and NIMLP were used as positive controls. The numbers of fraction below the circle (e.g. 12/12) represent the number of leaves showing cell death from the total number of treated leaves. TePDI-induced cell death occurs at 2 dpi and photographs were taken at 5 dpi and then leaves were stained with Trypan Blue. In B and E, detection of callose deposition and ROS accumulation in *N. benthamiana*. Leaves were infiltrated with *A. tumefaciens* carrying *TePDI* and *GFP* (B) or with purified 500-nM TePDI and EV proteins (E). Scale bar = 200 μm. EV indicates the empty vector control. DAB staining and Aniline Blue staining were performed 24 h after infiltration. In C and F, the relative expression of defense-related marker genes in *N. benthamiana* leaves. Leaves were collected at 24 h after transient expression of *TePDI* and *GFP* (C) or collected at 6 h after infiltration of purified 500-nM TePDI and EV proteins (F). Relative gene expression was normalized to *Nbrpl23* and calibrated to the levels of GFP or EV (set as 1). D, Leaves of eggplant, pepper, and tomato were infiltrated by *A. tumefaciens* carrying *TePDI*, *GFP*, and *INF1*. Asterisks represent statistically significant differences based on Student's *t* tests (*$P < 0.05$, **$P < 0.01$, ***$P < 0.001$); error bars represent SEM, $n = 3$.

inducing roles of TePDI by testing ROS burst and callose deposition. Transient expression of *TePDI* in *N. benthamiana* leaves was confirmed with western blot analysis (Supplemental Figure S1C). *TePDI* induced strong ROS and callose accumulation in *N. benthamiana* leaves (Figure 2B). In addition, the expression levels of SA-related genes (*NPR1* and *PR1a*) and JA-related genes (*PR3* and *PR4*) were significantly upregulated in leaves expressing *GFP-TePDI* relative to *GFP* (Figure 2C). To see if TePDI-induced cell death occurred in different species of plants, we transiently expressed TePDI in various plant leaves. As shown in Figure 2D, TePDI also induced cell death in tomato, eggplant (*Solanum melongena*), and pepper (*Capsicum annuum*), while INF1 only induced cell death in pepper and eggplant.

To confirm the ability of TePDI to trigger plant defenses, TePDI protein was expressed and purified from *Escherichia coli*, and was used to infiltrate *N. benthamiana* leaves (Supplemental Figure S1E). Again, more ROS accumulation and callose deposition were detected in TePDI-infiltrated leaves relative to those in the empty vector (EV)-infiltrated leaves (Figure 2E). In addition, transcript levels of SA-related genes (*NPR1* and *PR1a*) and JA-related genes (*PR3* and *PR4*) were significantly higher in purified TePDI-infiltrated leaves compared to the EV controls (Figure 2F). Together, these results indicate that TePDI is an elicitor that can induce plant defense responses.

The biological functions of TePDI during natural infestation of plants by *T. evansi* were also measured by testing how plants responded to *T. evansi* feeding after silencing *TePDI*. Reverse transcription quantitative–polymerase chain reaction (RT–qPCR) results showed that *TePDI* transcripts were significantly knocked down in ds*TePDI*-treated spider mites (Supplemental Figure S2). In *N. benthamiana* plants, infestation by *TePDI*-silenced mites significantly reduced the expression levels of SA genes (*NPR1* and *PR1a*) and the JA-related gene *PR3* (Figure 3A). Similarly, in tomato plants, the transcript levels of SA-related genes *PR1a* and *PR1b* (pathogenesis-related protein 1b) were also significantly lower in leaves infested by ds*TePDI*-treated mites than in control leaves infested by ds*RFP*-treated mites (Figure 3C), but not in JA-related genes *JIP21* (jasmonate-inducible protein-21) and *LOXD* (*lipoxygenase D*). In addition, we found the contents of H_2O_2 (endogenous ROS) in both *N. benthamiana* and tomato leaves after infestation by ds*TePDI*-treated mites were significantly lower than in the control treatments (Figure 3, B and D). These results supported the key functions of TePDI in inducing plant defense responses during spider mite feeding.

TePDI promotes plant resistance to *T. evansi*

To confirm that TePDI-induced plant defenses enhance plant resistance against herbivores, we checked the survival

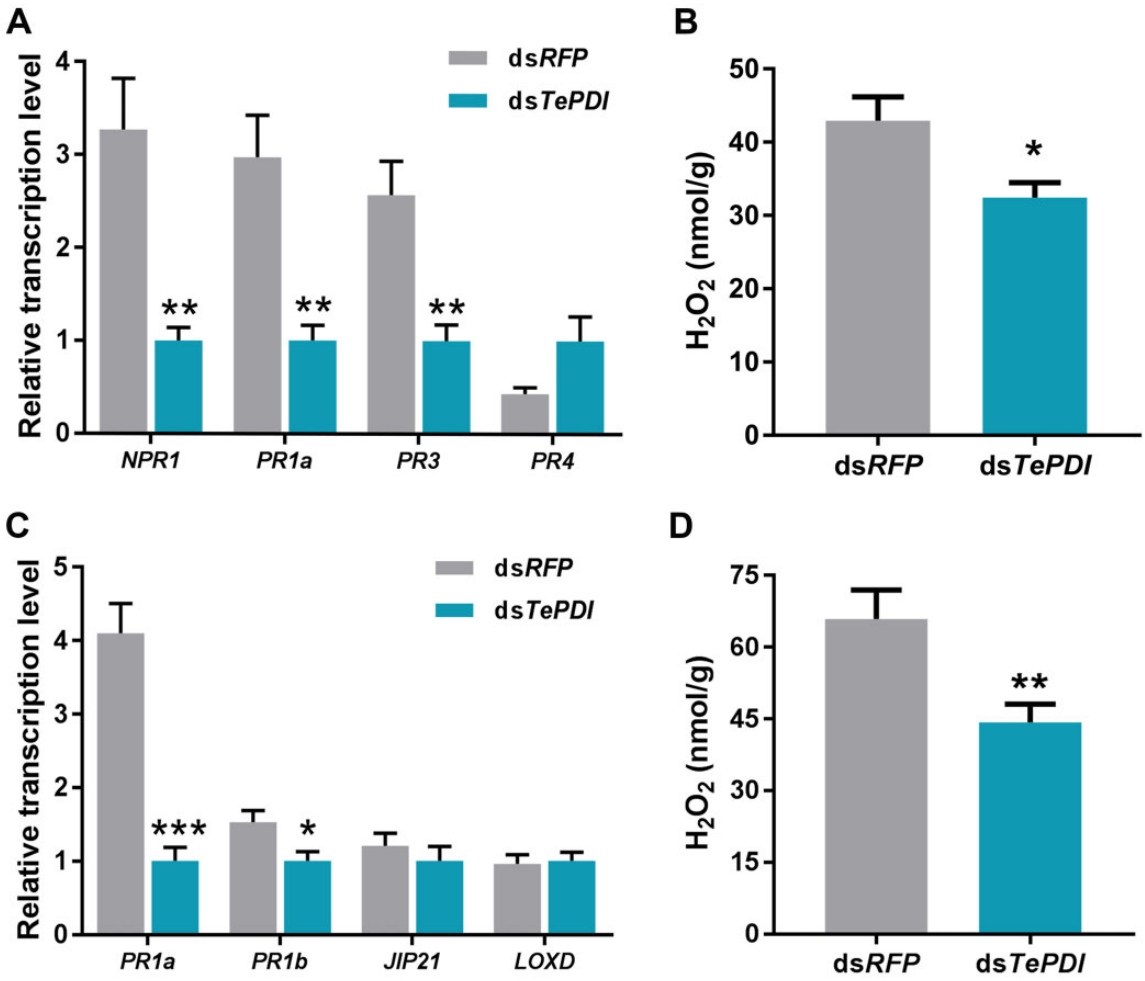

Figure 3 *TePDI*-silenced mites suppressed plant defense responses. A, C, Relative expression of SA-related genes (*NPR1*, *PR1a*, and *PR1b*) and JA-related genes (*PR3*, *PR4*, *JIP21*, and *LOXD*) in *N. benthamiana* (A) and *S. lycopersicum* (C) leaves that had been infested by dsRNA-treated spider mites for one day. In (B) and (D), the hydrogen peroxide (H_2O_2) content of *N. benthamiana* (B) and *S. lycopersicum* (D) leaves are plotted. *Nbrpl23* and *Slactin* genes were internal controls for RT–qPCR. Asterisks represent statistically significant differences based on Student's *t* test (*$P < 0.05$, **$P < 0.01$, ***$P < 0.001$); error bars represent SEM, $n = 3$.

and feeding preference of *T. evansi* on the *TePDI*-expressed or *GFP*-expressed *N. benthamiana* leaves. Transient expression of *TePDI* in *N. benthamiana* decreased the survival of spider mites compared with *GFP*-expressed leaves (Figure 4A). In a dual-choice assay, more spider mites fed on the *GFP*-expressed leaves relative to the *TePDI*-expressed leaves at multiple observation points (Figure 4B). Similarly, *T. evansi* had a lower survival on purified TePDI-treated leaves than on the EV-infiltrated leaves (Figure 4C). Spider mites preferred EV-infiltrated leaves as well (Figure 4D). In sum, TePDI-induced responses decreased the plant's attractiveness to, and survival of, spider mites.

TePDI-triggered cell death in *N. benthamiana* requires SGT1 and HSP90

To determine plant regulators associated with TePDI-mediated cell death, we knocked down the expression of PTI- and ETI-regulating genes with a virus-induced gene silencing (VIGS) assay in *N. benthamiana* (Figure 5A; Supplemental Figure S3A). RT–qPCR analysis revealed that the expression of these genes was considerably reduced in silenced plants compared with control plants (Supplemental Figure S3B). Unlike BAK1- and SOBIR1-dependent PAMP INF1, TePDI induced cell death in both *NbBAK1*- and *NbSOBIR1*-silenced leaves (Figure 5B), which means the TePDI-triggered cell death is independent of NbBAK1 and NbSOBIR1. We found many NLR protein-related signaling components, such as RAR1, NDR1, and EDS1, were also not required for TePDI-mediated cell death (Figure 5C). Only silencing *SGT1* and *HSP90* genes in *N. benthamiana* abolished TePDI-triggered cell death, suggesting that SGT1 and HSP90 are required for TePDI-induced cell death in *N. benthamiana*. In addition, the expression levels of *SGT1* and *HSP90* genes were both significantly upregulated after *T. evansi* feeding on *N. benthamiana* leaves (Supplemental Figure S3C). *Tetranychus evansi* survived better when feeding on *SGT1*- and *HSP90*-silenced leaves than on *GFP*-silenced leaves (Supplemental Figure S3D). Taken together, our results

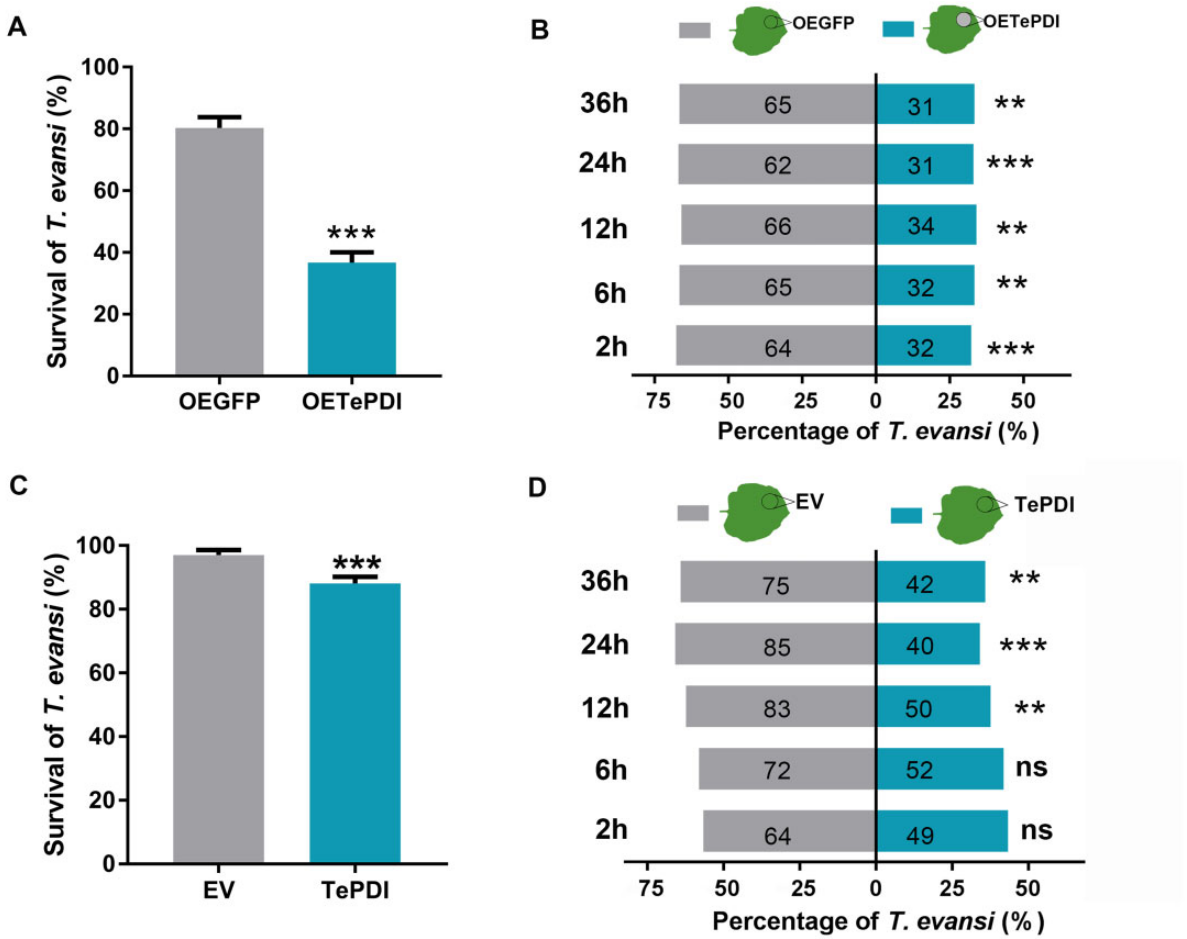

Figure 4 TePDI promotes plant resistance to *T. evansi*. A, Survival of *T. evansi* in *N. benthaimiana* leaves transiently expressing *TePDI* or *GFP* at 36 h after feeding ($n = 8$). B, Percentage of *T. evansi* choosing leaves transient expressing *TePDI* and *GFP* over different times ($n = 130$). C, Survival of *T. evansi* in TePDI protein-infiltrated or EV-infiltrated *N. benthamiana* leaves at 36 h after feeding ($n = 8$). D, Percentage of *T. evansi* choosing leaves infiltrated with TePDI and EV proteins over different times ($n = 165$). Asterisks represent statistically significant differences based on Student's *t* test or χ^2 test (**$P < 0.01$, ***$P < 0.001$); ns, not significant. Error bars represent SEM.

suggest that plants may deploy SGT1 and HSP90 to recognize TePDI and induce resistance to *T. evansi*.

Effectors of *T. evansi* suppress TePDI-triggered plant defenses

Since *T. evansi* can successfully infest *N. benthamiana*, we hypothesized that the defense responses triggered by TePDI, including cell death, can be suppressed by *T. evansi* effectors. To test this hypothesis, we transiently expressed known *T. evansi* effector proteins and measured whether they could suppress TePDI-induced responses in *N. benthamiana*. As shown in Figure 6A, effectors Te84 (MH979724) and Te28 (KT156789) substantially inhibited TePDI-mediated cell death, whereas the GFP control and the remaining effectors did not. Similarly, ROS burst and callose deposition triggered by TePDI could be suppressed by transiently expressing *Te28* and *Te84* in *N. benthamiana* (Figure 6, B and C). Furthermore, relative to GFP, Te28 and Te84 reduced the TePDI-induced gene expression of *NPR1*, *PR1a*, *PR3*, and *PR4*, though it was not significantly different for *NPR1* and *PR1a* (Figure 6, D and E). In contrast, Te19 (MH979721) and Te128 (MH979711) failed in suppressing plant defenses triggered by TePDI (Figure 6, F and G). These data indicate that TePDI-induced immunity can be neutralized by spider mite effectors.

Functioning of TePDI requires thioredoxin domains a, b, and b′

TePDI has four thioredoxin domains (a, b, b′, and a′) and an ER retention signal (KDEL). To define the key regions required for the cell death-inducing activity of TePDI, we generated a series of deletion mutants (Figure 7A). Only the mutant with deleted a′ continued to trigger cell death, indicating that the three domains (a–b–b′) are required for TePDI to induce cell death. Subcellular localization assays showed that the green fluorescent signals representing TePDI with the signal peptide exclusively localized at the plasma membrane (Supplemental Figure S4), while TePDI without signal peptide and other deletion mutants localized at the nucleus and cytoplasm (Figure 7B). Intriguingly,

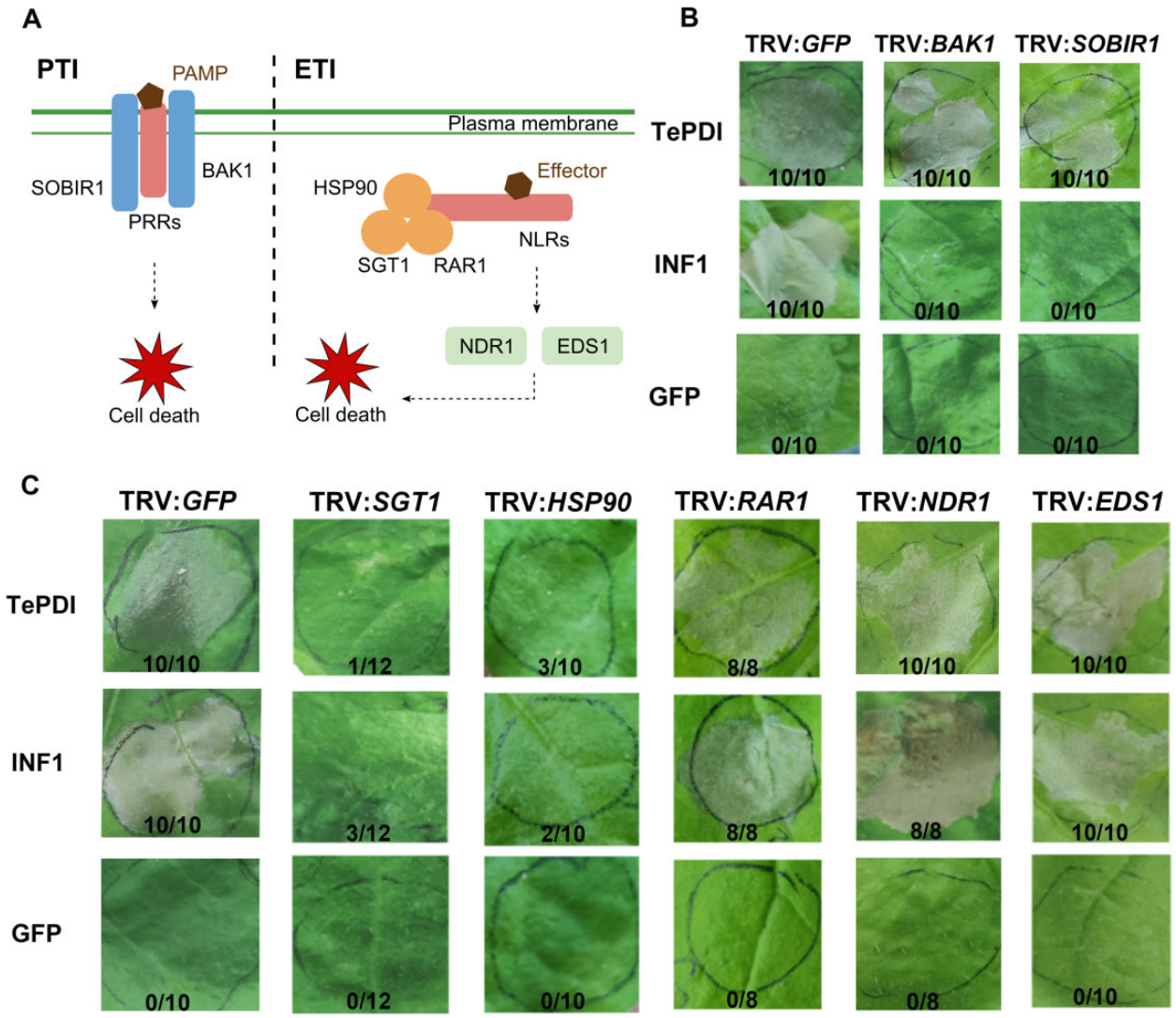

Figure 5 SGT1 and HSP90 are required for TePDI-mediated cell death in *N. benthamiana*. A, The model diagram of PTI- and ETI-mediated immunity. PTI is activated when PAMPs are recognized by PRRs that are interacting with BAK1 and SOBIR1 on the membrane of plant cells. For ETI, effectors are recognized by intracellular NLRs, which require the chaperone complex (HSP90–SGT1–RAR1). The EDS1 and NDR1 are necessary for NLRs-mediated immune responses. B, C, Transient expressing *TePDI* in *GFP-*, *BAK1-*, *SOBIR1*-silenced *N. benthamiana* leaves (B) and in *GFP-*, *SGT1-*, *HSP90-*, *RAR1-*, *NDR1-*, and *EDS1*-silenced *N. benthamiana* leaves (C). GFP and INF1 were the controls. The numbers of fraction below the circle (e.g. 10/10) represent the number of leaves showing cell death from the total number of treated leaves. *Agrobacterium* was infiltrated at an OD_{600} of 0.3 and photographs were taken at 5 dpi.

another PDI family member in *T. evansi*, named TePDI2, did not induce cell death when transiently expressed in *N. benthaminana* (Figure 7C). TePDI2 also possesses a signal peptide, four thioredoxin domains, and ER retention signal. However, TePDI2 shared only 33% protein sequence similarity with TePDI (Supplemental Figure S5). Protein sequence alignments indicate that the sequence similarity of the b and b′ domains of TePDI compared to those of TePDI2 is relatively low (Supplemental Figures S5 and Figure S6).

Arthropod PDIs are highly conserved in activating plant defenses

The finding that TePDI-induced cell death is present in many plant species suggests that dialog between TePDI and plants may be ancient. We therefore analyzed the phylogeny and evolutionary rate of CDS of this protein across arthropods. PDI homologs are clustered in distinct groups that follow the broader arthropod groupings of Arachnida (spiders, ticks, and mites), Malacostraca (crabs, shrimps, lobsters and isopods), and Insecta (insects; Supplemental Figure S7). Protein sequence alignments show that PDI domains are conserved among various groupings of arthropods (Supplemental Figure S6). These results suggest that PDI is an ancient and conserved protein across the arthropods.

Transient expression assay showed that, apart from TePDI, PDIs from other *Tetranychus* species of spider mites, *T. urticae* and *T. truncatus*, also induced cell death and ROS burst in *N. benthamiana* leaves (Figure 8B), suggesting that PDIs

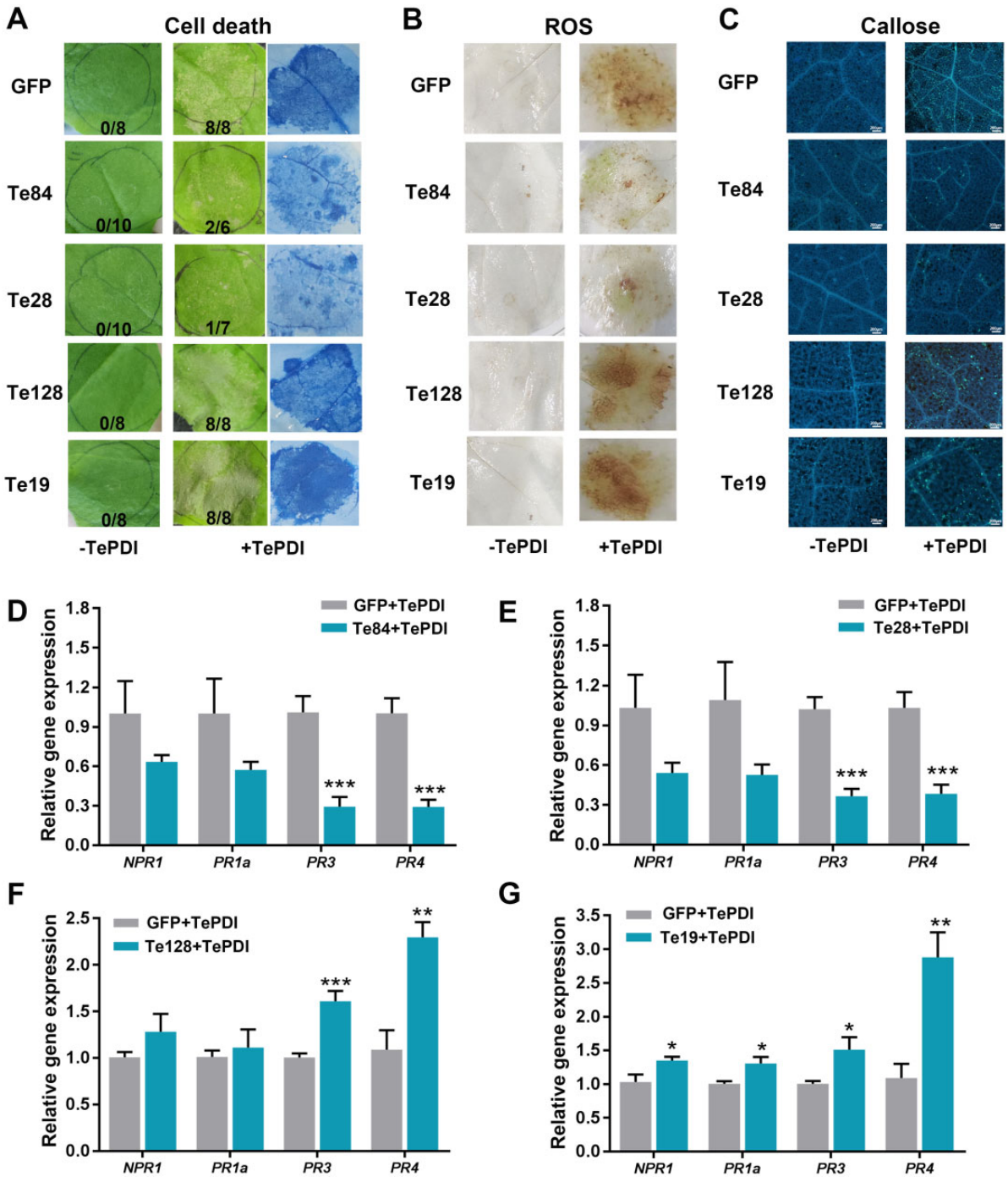

Figure 6 Suppression of TePDI-mediated cell death and defense responses by *T. evansi* effectors. A, Suppression of TePDI-induced cell death in *N. benthamiana* leaves by agroinfiltration of *T. evansi* effectors or GFP. +TePDI and −TePDI indicate leaves agroinfiltrated with and without *TePDI* respectively at 24 h after effector agroinfiltration in the same area. Leaves were photographed at 3 dpi and then stained with Trypan Blue. The numbers of fraction below the circle (e.g. 8/8) represent the number of leaves showing cell death from the total number of treated leaves. B, C, Suppression of TePDI-induced ROS (B) or callose deposition (C) in *N. benthamiana* leaves by agroinfiltration of *T. evansi* effectors. Scale bar = 200 μm. D–G, The transcript level of PR-related genes in the *N. benthamiana* leaves. Leaves were agroinfiltrated with candidate effectors Te84 (D), Te28 (E), Te128 (F), Te19 (G), or *GFP* and 24 h later in the same area with *TePDI*, and then were collected 24 h after TePDI treatment. Relative gene expression was normalized to *Nbrpl23* and calibrated to the levels of GFP (set as 1). Asterisks represent statistically significant differences based on Student's *t* test (*$P < 0.05$, **$P < 0.01$, ***$P < 0.001$). Error bars represent SEM, $n = 6$.

may have important primary physiological functions that outweigh the costs of inducing cell death and/or the maintenance of effectors. Because LsPDI1 from the plant sap-sucking insect *L. striatellus* also induces plant defense (Fu et al., 2021), we hypothesized that the ability of plants to detect PDI is a broad-spectrum trait. We therefore cloned

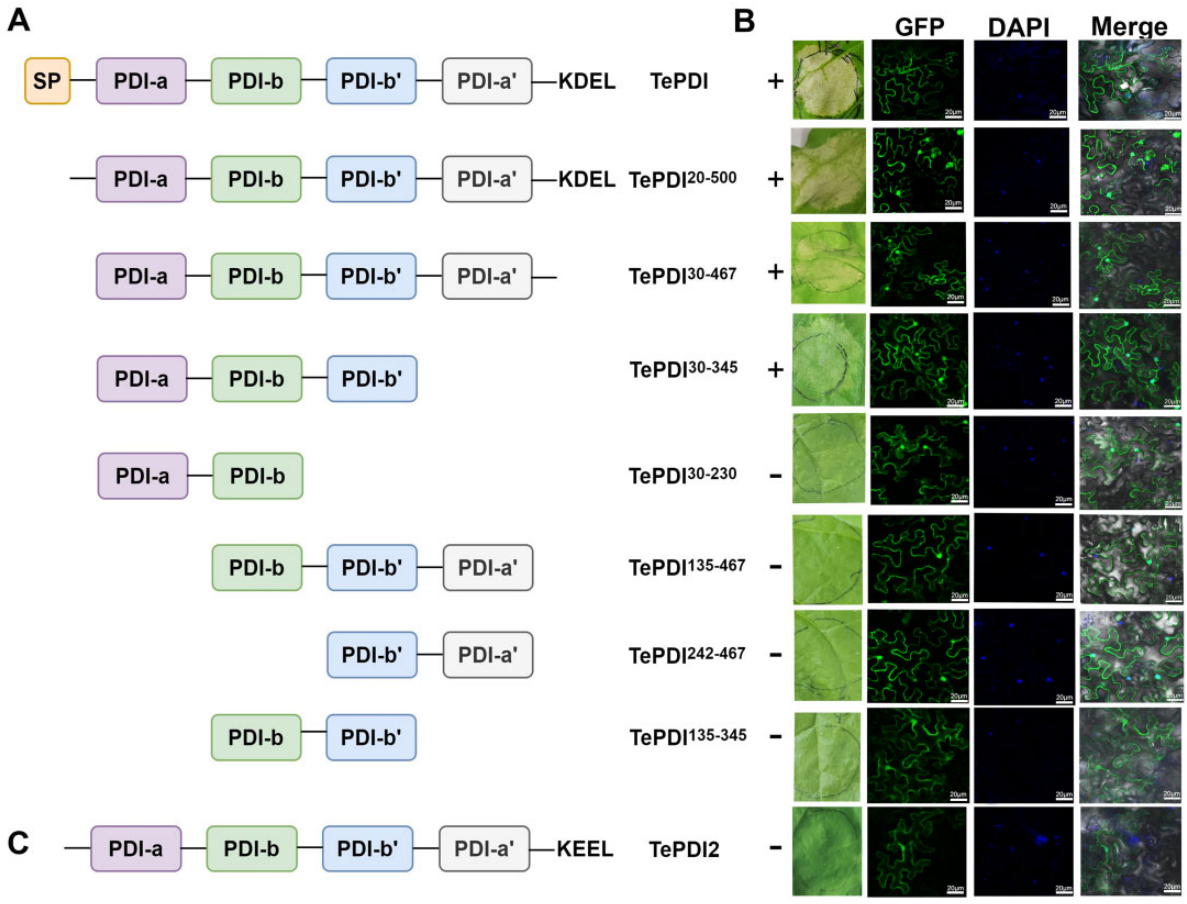

Figure 7 Functional domain analysis of TePDI. A, Schematic illustrations of TePDI and the deletion mutants. SP represents signal peptide; PDI-a, -a′, -b, and -b′ represent four thioredoxin structural domains; KDEL is the retention signal of ER. B, Cell death symptoms and subcellular localization in *N. benthamiana* leaves expressing TePDI deletion mutants. + and – represent the presence and absence of cell death symptoms. Green fluorescence signals (GFP) refer to the localization of truncated PDI proteins. Blue fluorescence signals (DAPI) refer to the cell nucleus. Fluorescence signals were observed at 488 nm (GFP) and 405 nm (DAPI) by confocal laser-scanning microscopy. Scale bar = 200 μm. C, Schematic illustration for structural domains of TePDI2.

the *PDI* gene from a wide range of feeding guilds (Figure 8A) including *Bemisia tabaci*, a Hemipteran pest that sucks plant phloem sap, *Spodoptera frugiperda*, a Lepidopteran pest that chews on plant leaves, *Drosophila melanogaster*, a Dipteran insect that feeds on spoiled fruits, *Anopheles stephensi*, a Dipteran pest that sucks mammalian blood, and *Haemaphysalis longicornis*, an Acaria tick that sucks mammalian blood. Our results showed that, despite having different feeding modes, the herbivorous *B. tabaci* and *S. frugiperda* both had PDIs that triggered cell death and ROS accumulation. Intriguingly, PDI homologs in saprophagous flies (fruit flies) and sanguivorous arthropods (ticks and mosquitoes) also triggered plant defense responses (Figure 8B), even though the PDIs of these species may never come in contact with live plant cells. In addition, DmPDI and SfPDI more strongly induced the expression of PR-related genes (*NPR1*, *PR1a*, *PR3*, and *PR4*) than the GFP control (Supplemental Figure S8). These findings indicate that PDI being perceived as a HAMP by plants is not limited to herbivores but extends to other nonphytophagous arthropods.

To gain insights into selection patterns on PDI, we computed ω (dN/dS) values, which indicate the ratio of nonsynonymous (dN) to synonymous (dS) substitution rates. The codeml program from the PAML package showed the global dN/dS of PDI among arthropods to be 0.067 ($\ll$1) (Supplemental Figure S7). We examined the null and alternative models of codon substitutions [M1a versus M0, M1a versus M2a, and M7 versus M8] (Supplemental Table S2). All models indicated that the dN/dS value was very small and that positive selection sites were absent. We also analyzed 496 single-copy ortholog groups from 15 published genomes of Arachnida and Insecta members (Figure 8A) and found a dN/dS value of *PDI* smaller than that of 78.2% of genes that encode conserved single-copy putative orthologs (Figure 8C). These results suggest that PDI has evolved under strong purifying selection, and also point to the likely importance of PDIs in core arthropod biological processes.

PDIs are required for herbivore performance

To obtain more insights into PDI, we analyzed the expression pattern of *TePDI* in *T. evansi*. *TePDI* was expressed

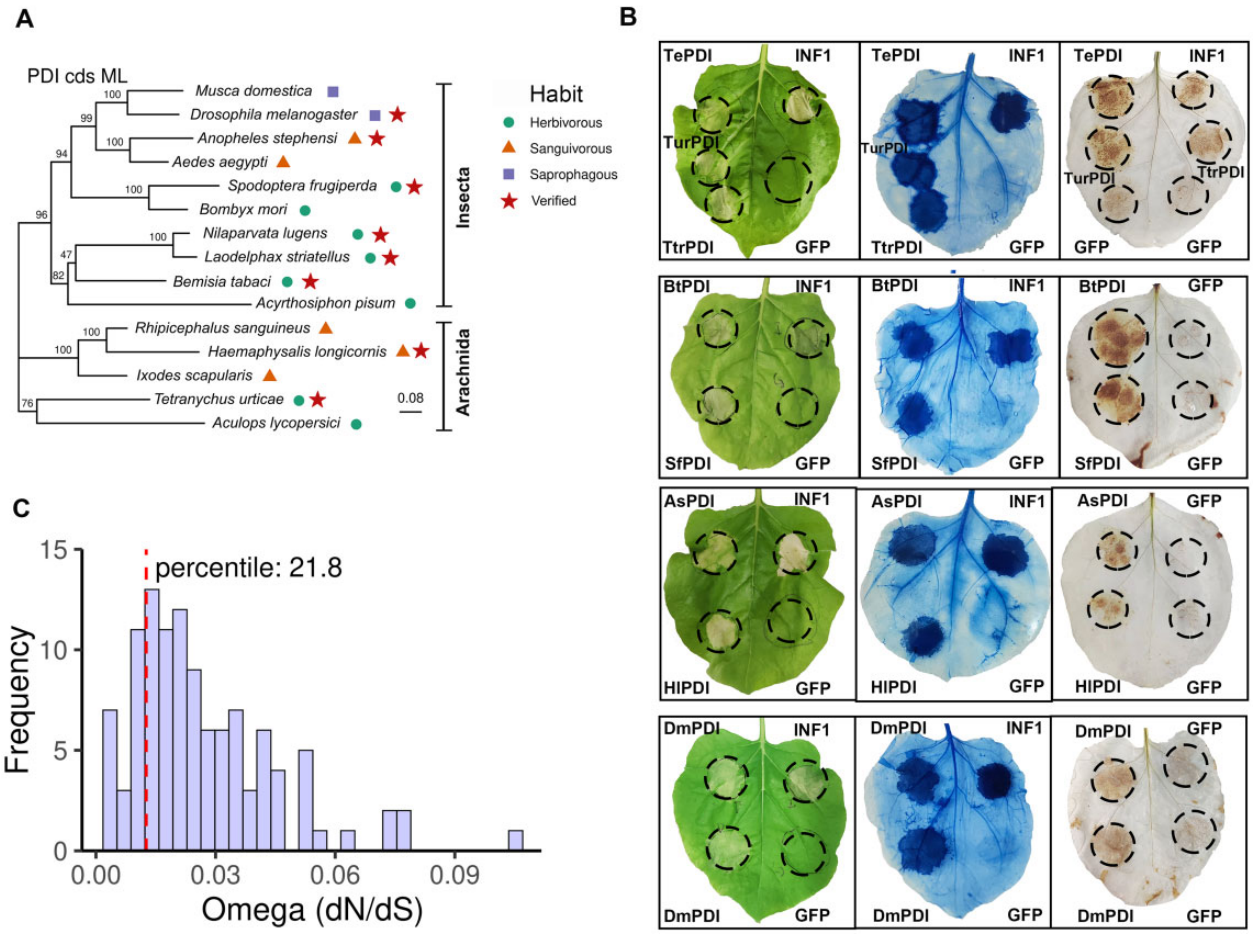

Figure 8 Conserved function of arthropod PDIs in inducing plant defenses. A, Phylogenetic analysis of TePDI and the homologous proteins from 15 representative arthropod species. Bootstrap percentage values are indicated on the branches. Scale bar indicates a 0.08-nucleotide substitutions per site. The proteins that have been validated for function in *N. benthamiana* are indicated by a red star. B, The homologous proteins of TePDI induced cell death and ROS accumulation. TePDI homologs from *T. urticae* (TurPDI), *T. truncatus* (TtrPDI), *B. tabaci* (BtPDI), *S. frugiperda* (SfPDI), *A. stephensi* (AsPDI), *H. longicornis* (HlPDI), and *D. melanogaster* (DmPDI) were transiently expressed in *N. benthamiana*. C, Distribution of dN/dS values of genes encoding single-copy putative orthologs across the 15 arthropod genomes. The vertical red dotted line represents the value for *PDI* with actual percentile ranks.

across the life stages of *T. evansi* and its transcripts did not differ in the posterior and anterior parts of its body (Figure 9, A and B). Whole-mount fluorescence *in situ* hybridization results showed that *TePDI* was expressed in the anterior prosomal glands and other parts of the *T. evansi* body (Figure 9C), while the negative control (sense probe) did not hybridize with any tissues (Figure 9D). This implies that TePDI is not only a salivary protein but may also be required for mite development. To test whether PDI is important for herbivore biology, we performed RNAi on *T. evansi* and *B. tabaci* and were successful in knocking down *PDI* transcripts in both species (Supplemental Figure S9A). Spider mites treated with ds*TePDI* showed significantly lower fecundity and lower survival than the ds*RFP* control group (Figure 9, E and F). Similarly, the survival rate of *BtPDI*-silenced whiteflies significantly decreased after 4 days of dsRNA treatment (Supplemental Figure S9B), although no significant difference in fecundity was detected between ds*RFP*- and ds*BtPDI*-fed whiteflies (Supplemental Figure S9C). These results point to the importance of PDIs in herbivores for survival and for maintaining reproductive performance.

Discussion

Recent in-depth genomic and proteomic analyses have provided growing evidence that HAMPs affect numerous processes in plants (Rao et al., 2019). In this study, we show that PDI is a protein conserved across arthropods that diverged more than 2.5 million years ago and that PDI putative orthologs are generally perceived as HAMPs by plants, triggering defense reactions. Our results help to build an understanding of how plants recognize herbivores, and how herbivores in turn suppress them. The results also provide insights into the interplay between HAMPs and effectors during plant–herbivore co-evolution.

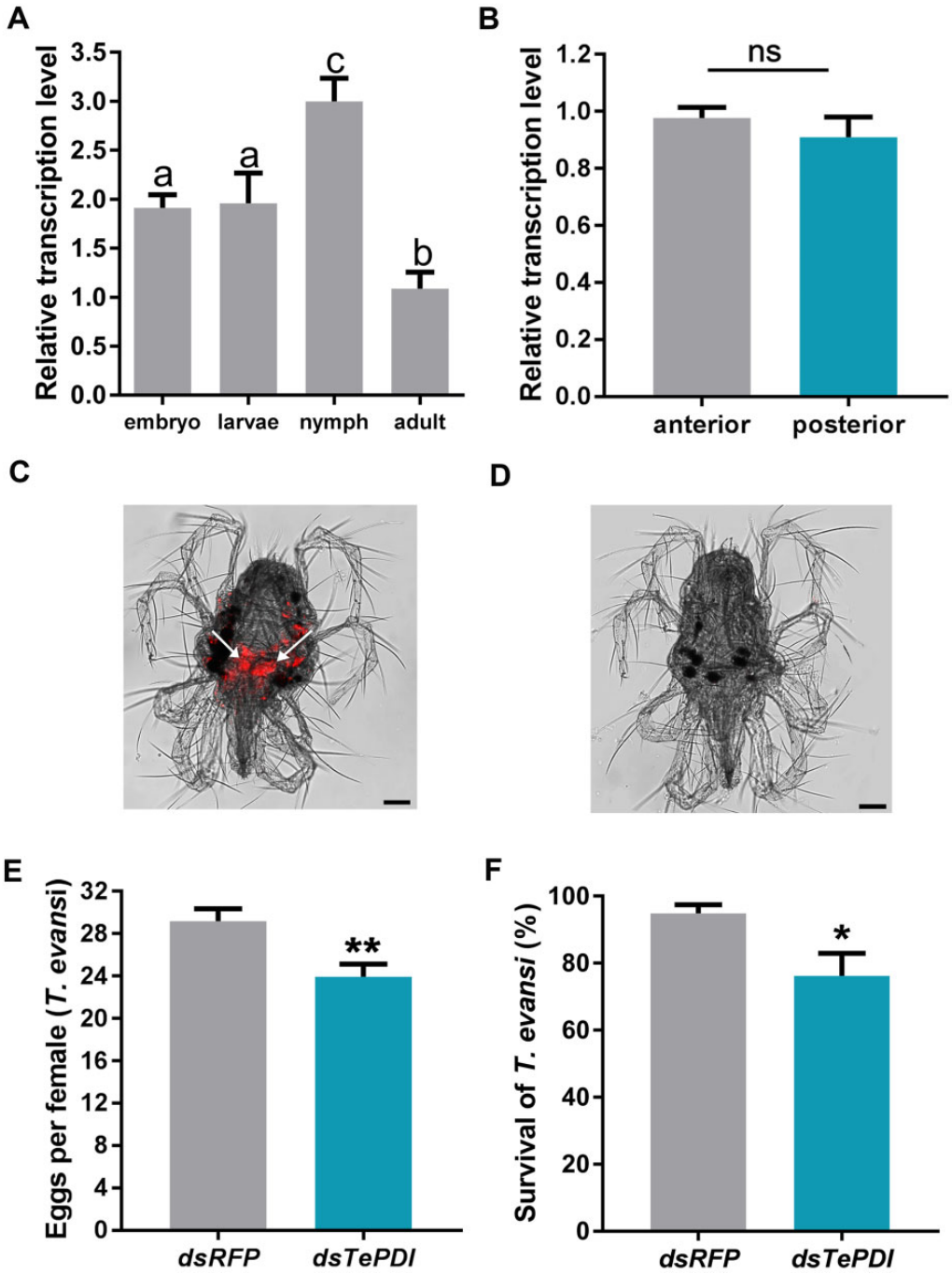

Figure 9 TePDI is required for normal performance of *T. evansi*. Relative expression abundance of *TePDI* at different developmental stages (A) and different tissues (B) in *T. evansi*. The *TeATPase* gene was selected as the internal control. $n = 6$. C and D, Whole-mount fluorescence *in situ* hybridization of *TePDI* transcripts in *T. evansi*. Spider mites were hybridized with digoxigenin (DIG)-labeled antisense probe and FastRed as substrate. The fluorescent signals represent the location of *TePDI* (C). The anterior salivary glands were indicated by arrows. Sense probe of *TePDI* was used as the negative control (D). Scale bar = 50 μm. E and F, The fecundity and survival rate of dsRNA-treated spider mites. The ds*RFP*-treatment was the control. n = 26. Different letters indicate statistically significant difference following a one-way ANOVA and Tukey's post hoc test ($P < 0.05$). Asterisks at the top of the bars indicate statistically significant differences based on Student's *t* tests (*$P < 0.05$, **$P < 0.01$, ***$P < 0.001$); ns, not significant. Error bars represent SEM.

Consistent with a previous report (Paulo et al., 2018) showing that *T. evansi* suppressed plant defenses in tomato and bean, but activated defenses in tobacco (*N. tabacum*), our results showed that *T. evansi* infestation significantly upregulated the expression levels of SA- and JA-related genes in *N. benthamiana*. This suggests that *T. evansi* may activate *N. benthamiana* defense responses by releasing salivary proteins. After screening several salivary proteins, we

identified TePDI, which strongly induced cell death, ROS accumulation, and callose deposition in *N. benthamiana* leaves (Figures 2 and 3). ROS accumulation and callose deposition are induced by herbivores and recognized as signaling molecules of plant defense deployment (Shangguan et al., 2018). Furthermore, TePDI induced the expression of genes associated with SA and JA signaling pathways (Figures 2 and 3), which participate in the interaction between *T. evansi* and plants (Alba et al., 2015). Overall, the recognition of TePDI enhanced *N. benthamiana* resistance to *T. evansi* (Figure 4).

TePDI is a secreted spider mite HAMP probably originating from their saliva. The defense reaction elicited by TePDI shares common features with defense responses shown by well-known PAMPs (Ma et al., 2015; Nie et al., 2019). In particular, TePDI-mediated plant defense requires SGT1 and HSP90 (Figure 5), which play key roles in plant recognition of PAMPs (Bos et al., 2006; Nie et al., 2019). SGT1 and HSP90 are structurally and functionally conserved (co-)chaperone complexes and are involved in plant resistance against aphids and whiteflies (Bhattarai et al., 2007). Our results demonstrated that knocking down *SGT1* and *HSP90* decreased plant resistance to spider mites. Thus, we speculate that resistance against herbivores produced by *SGT*1 and *HSP90* may be broad-spectrum. In addition, SGT1 and HSP90 are key elements in plant perception of pathogens (Shirasu, 2009). SGT1 and HSP90 are also required for the activation of cell death by pathogen effectors PiNPP1.1 and AVR3a in *Phytophthora infestans*, as well as PAMPs INF1 and VmE02 (Bos et al., 2006; Kanneganti et al., 2006; Nie et al., 2019). These findings suggest that SGT1 and HSP90 are hubs in plant defense networks and imply that PAMP-triggered and ETI are tightly associated (Yuan et al., 2021). However, TePDI-mediated cell death is not dependent on the plant co-receptors BAK1 and SOBIR1, indicating that TePDI may be recognized by other co-receptors on the cell membrane, or possibly be recognized by plant pathways distinct from PAMP recognition.

The interaction between herbivores and plants is an example of a "predator-prey" type model, where both parties evolve to counter each other's evolutionary changes. To deal with plant defenses, herbivores have evolved mechanisms to secrete effectors that inhibit HAMP-triggered immunity and thereby facilitate their utilization of plants. Our results show that effectors Te28 and Te84 can inhibit cell death and defense responses triggered by TePDI (Figure 6). Te28 and Te84 were previously reported to inhibit SA and JA response and promote spider mite fecundity in *N. benthamiana* (Villarroel et al., 2016; Schimmel et al., 2017). In addition, some effectors are conserved in plant-sap sucking species, such as the effector Armet in aphids and whiteflies (Cui et al., 2019; Du et al., 2022), Mp10 homologs in diverse plant-sap sucking insect species and earlier diverged species (Drurey et al., 2019), and Te28 in spider mites (Villarroel et al., 2016). This suggests that some effectors may have evolved to manipulate conserved plant targets and, possibly in concert with host-specific effectors, to counteract conserved HAMP-recognition mechanisms of plants. This leads to a complex co-evolutionary scenario involving broad-spectrum surveillance mechanisms to detect conserved HAMPs as well as conserved and dedicated effector repertoires to bypass such detection.

Deleting the signal peptide did not affect TePDI-induced cell death; the thioredoxin domain a is more important than a′ for activating plant cell death (Figure 7), suggesting that the functions of a and a′ are not redundant in TePDI. These results are similar to results obtained in the oomycete *P. parasitica* and the nematode *Globodera pallida* (Meng et al., 2015; Gross et al., 2020), but are contrary to those in LsPDI1 (Fu et al., 2021), even though the PDI from *L. striatellus* (*LsPDI1*) is phylogenetically closer to *TePDI*. The TePDI2 harbored a, b, b′, and a′ domains, but failed to induce plant cell death (Figure 7C), possibly because the b and b′ domains of TePDI and TePDI2 differed substantially, suggesting that the noncatalytic domains are important for PDI functioning.

The functional importance of PDI proteins is evident in many eukaryotes, including plants, pathogens, and arthropods. In *Arabidopsis thaliana*, PDIs play a role in oxidative protein folding and secretion (Fan et al., 2022). In nematodes, MiPDI protects *M. incognita* from oxidative stress (Zhao et al., 2020). In ticks, HlPDI is critical for *H. longicornis* biology and might be involved in blood-feeding (Liao et al., 2007). Our functional results show that TePDI is required for maximal herbivore performance on plants, given that knockdown of the *PDI* gene reduced the survival of adults of both *T. evansi* and *B. tabaci* (Figure 9). Similarly, NIMLP from *N. lugens* is a HAMP that not only triggers plant immune responses but also acts as a key salivary protein for the formation of a salivary sheath (Shangguan et al., 2018). These examples suggest that HAMPs have beneficial primary functions in plant-feeding arthropods that outweigh the costs of them being perceived as HAMPs by plants.

We demonstrated that not only PDI from herbivores but also from nonherbivores are perceived as HAMPs by plants and elicit defense responses (Figure 8), although many of them may never interact with plant cells in nature. This probably relates to the conserved regions of PDIs being recognized by plants. Apart from *N. benthamiana*, TePDI also triggers cell death in other Solanaceae plants including tomato, eggplant, and pepper (Figure 2), suggesting that PDIs may be recognized by Solanaceae plants via a conserved mechanism. Our results support the notion that various plants detect conserved HAMPs, thereby reducing the need for parallel more dedicated surveillance mechanisms.

In conclusion, we have shown PDI to be conserved across phytophagous and nonphytophagous arthropods and to be generally perceived by plants as a HAMP. In particular, TePDI elicits cell death in diverse plant species. This indicates that plants target conserved elements in this HAMP. TePDI-induced cell death depends on the plant signaling molecules SGT1 and HSP90. Interestingly, defense induction by TePDI in *N. benthamiana* is counteracted by the mite's

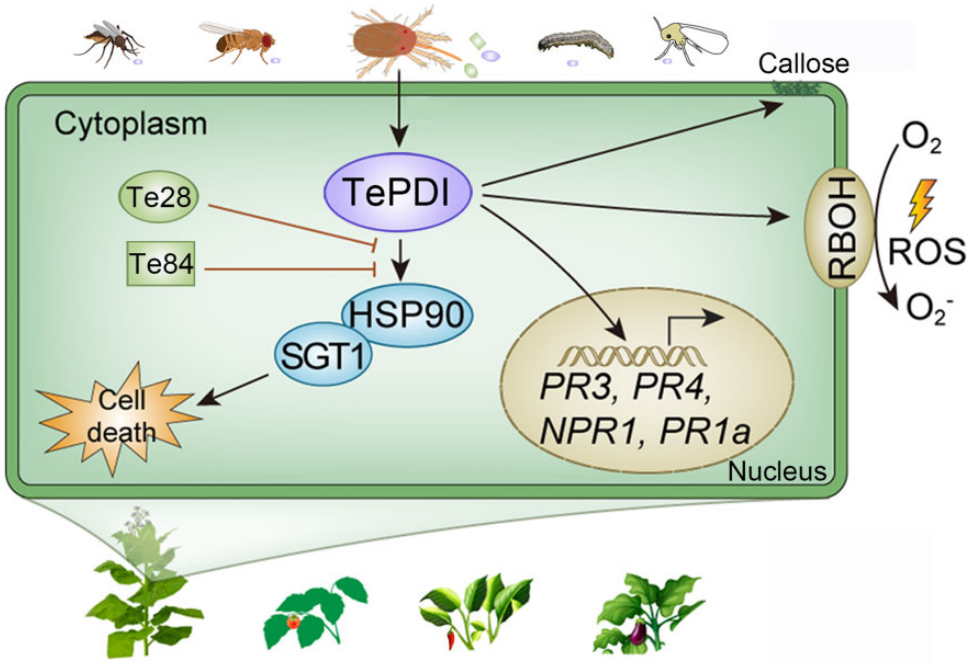

Figure 10 Working summary of TePDI involvement in plant–herbivore interaction. PDI as a HAMP is broadly conserved in phytophagous and nonphytophagous herbivores. AsPDI from *A. stephensi*, DmPDI from *D. melanogaster*, BtPDI from *B. tabaci*, and SfPDI from *S. frugiperda* can all activate plant immunity. When *T. evansi* feeds on leaves, TePDI can be secreted into plant cells and induces defense responses in a wide range of plants, including *N. benthamiana*, tomato, pepper, and eggplant. This elicited defense response is dependent on the plant signaling molecules SGT1 and HSP90. However, to improve performance, *T. evansi* suppresses TePDI-induced responses by secreting effectors Te28 and Te84. ROS, reactive oxygen species; SGT1, suppressor of the G2 allele of skp1; HSP90, heat shock protein 90; NPR1, nonexpressor of pathogenesis-related genes 1; PR1a, pathogenesis-related protein 1a; PR3, pathogenesis-related protein 3; PR4, pathogenesis-related protein 4.

salivary effectors Te28 and Te84 (Figure 10). Further studies are needed to explore how PDIs are perceived by plants and how they activate plant immunity through exploring corresponding plant receptors. We speculate that resistance breeding should aim for mechanisms that detect conserved HAMPs/PAMPs and stack these in crops (like they do with R genes) to obtain broad-spectrum resistance while minimizing the opportunity for herbivore effectors to undo detection.

Materials and methods

Plants and arthropods husbandry

Tomato (*Solanum lycopersicum*), eggplant (*Solanum melongena*), pepper (*Capsicum annuum*), and *N. benthamiana* were grown in climate chambers at 25°C ± 1°C, 16-light photoperiod and 60% ± 10% relative humidity.

The tomato red spider mite (*Tetranychus evansi*) was obtained from tomato plants in Ya'an, Sichuan Province, China, in 2016, and was cultured on tomato plants in a transparent storage box. The box was kept in a tray filled with water to prevent mites from escaping and invasion of other arthropods. The MED whitefly (*Bemisia tabaci*) was collected from tomato plants in Nanjing, Jiangsu Province, China, in 2017, and was maintained on tomato plants in insect-proof cages. Species identification of spider mite and whitefly were conducted with the molecular markers nuclear ribosomal internal transcribed spacer *ITS* (AB738755.1) and mitochondrial cytochrome oxidase subunit 1 *mtCOI* (MH908652), respectively. The primer sequences are listed in Supplemental Table S3. All herbivores were reared in a growth chamber with 60% ± 5% relative humidity under a 16-light photoperiod at 25°C ± 1°C.

Defense responses induced by *T. evansi* infestation in *N. benthamiana*

Nicotiana benthamiana leaves were divided along the main leaf veins by insect glue (The Scotts Miracle-Gro Company, Marysville, OH, USA) to produce two sides. One side was infested with 30 *T. evansi* adults, while the other uninfested side served as the control.

To measure ROS in plants, the leaves were cut and immersed in a solution containing 1 mg/mL^{-1} 3,3-diaminobenzidine (DAB) for 12 h. After removing the DAB-HCl (PH = 3.8) solution, leaves were destained with ethanol. The final brown color of the leaf is an indicator of ROS accumulation (Huang et al., 2019b).

Callose deposition in the leaves was detected by Aniline Blue staining as described previously (Shangguan et al., 2018). Stained samples were viewed under a Olympus IX71 fluorescent microscope (Olympus, Tokyo, Japan). Fluorescence was observed under ultraviolet light (wavelength = 405 nm). The staining shows callose deposition as blue dots. To quantify the content of H_2O_2 in leaves, we used a Hydrogen Peroxide Assay Kit (Beyotime, Haimen,

China). The leaves were lysed by exposure to a lysis solution for 30 min at 30°C. Absorbance at A560 was read by a microplate reader.

To explore the expression of SA- and JA-related genes in leaves, we collected total RNA from the treated leaves as described above and reverse transcribed 1-μg RNA using HiScript II QRT SuperMix (Vazyme). RT–qPCR was performed on an ABI 7500 Real-Time PCR System (Applied Biosystems, Carlsbad, CA, USA) with ChamQ Universal SYBR qPCR Master Mix (Vazyme). The housekeeping genes *Nbrpl23* and *Slactin* were used as reference control genes for *N. benthamiana* and tomato (*S. lycopersicum*), respectively. Relative expression levels were calculated using the $2^{-\Delta\Delta Ct}$ method. The primer sequences designed with Primer Premier (v6.00) are listed in Supplemental Table S3. At least three biologically independent replicates were performed for each sample.

Bioinformatics analysis

All sequences were translated into proteins and their molecular masses were predicted by the Expasy Server (Gasteiger et al., 2003). Signal peptides and their cleavage sites in PDI proteins were predicted by SignalP 5.0 (Armenteros et al., 2019). Transmembrane domains were predicted using THMMM v2.0 (Krogh et al., 2001). The corresponding NCBI accession numbers of PDI genes are listed in Supplemental Table S4. Conserved domains were predicted by the NCBI CD search program (https://www.ncbi.nlm.nih.gov/Structure/cdd/wrpsb.cgi).

Cloning *PDI* genes from arthropods

Total RNA was extracted from adults of *Tetranychus evansi*, *T. urticae*, *T. truncatus*, *B. tabaci*, *Spodoptera frugiperda*, and *Drosophila melanogaster* with Trizol (Invitrogen, Carlsbad, CA, USA) following the manufacturer's recommendations. cDNA was generated using HiScript II Q RT SuperMix for qPCR (+ gDNA wiper; Vazyme Biotech, Nanjing, China). The cDNA of *Anopheles stephensi* and *Haemaphysalis longicornis* was prepared from mosquito adults and tick nymphs, respectively. The CDS of candidate genes was amplified from cDNAs with PCR using the 2 × Phanta Max Master Mix (Vazyme) and was then ligated to the KpnI/XbaI-digested pBINGFP2 vector or SmaI digested pBINHA vector by Trelief SoSoo Cloning Kit (Tsingke, Beijing, China) according to the previous reference (Huang et al., 2019b). pBINHA encodes an HA tag attached to the C-termini of the proteins, while pBINGFP2 encodes GFP attached to the N-termini of the proteins. Information of arthropods is listed in Supplemental Table S5. The specific primers are listed in Supplemental Table S3.

Transient expression of *PDI* genes in *N. benthamiana*

The constructed vectors were introduced into *A. tumefaciens* strain GV3101 by electroporation. After confirming bacteria that were successfully transformed with PCR, the transformants were cultured in LB liquid medium with kanamycin and rifampicin for 24 h at 28°C. Recombinant strains were washed three times with infiltration buffer (1-M $MgCl_2$, 100-mM MES, 150-mM acetosyringone) and resuspended to OD_{600} (optical density near the 600 nm wavelength) = 0.4. The *Agrobacterium* cell suspension was injected into leaves of 4- to 6-week-old *N. benthamiana* plants with a needleless syringe. At 24-h post infiltration (hpi), agroinfiltrated *N. benthamiana* leaves were collected for plant defense-related assays. NIMLP and INF1, the previously characterized cell death-inducing proteins from brown planthopper *Nilaparvata lugens* (Shangguan et al., 2018) and plant pathogen *Phytophthora infestans* (Bos et al., 2006), respectively, were used as positive controls, while GFP was the negative control. *NIMLP* gene was ligated into vector pBINGFP2, while *INF1* was ligated into vector pBINHA. The dead cells were quantified by Trypan blue staining (Fernández-Bautista et al., 2016).

To test whether *T. evansi* effectors suppress TePDI-induced cell death, *N. benthamiana* leaves were first infiltrated with *A. tumefaciens* carrying candidate effector genes or green fluorescent protein (*GFP*), respectively. TePDI was injected in the same region after 24 h. The injected leaves were photo-recorded at 3-day post-infiltration (dpi). The ROS accumulation, callose deposition, and induction of defense-marker genes were detected 24 h after TePDI infiltration using above methods.

Protein expressing and infiltration assays

The CDS of TePDI without signal peptide was amplified and cloned into the pGEX-6P-1 expression vector. The recombinant protein was expressed in *E. coli* strain BL21 (DE3) with 1-mM IPTG for induction at 20°C for 24 h. Cells were collected by centrifugation and resuspended in phosphate-buffered saline (PBS; pH = 7.5). The suspended cells were lysed by sonication and the supernatant was obtained by centrifugation at 10,000*g* for 10 min. The supernatant containing TePDI protein was purified using AKTA Avant 25 (GE Healthcare, Chicago, IL, USA) following the manufacturer's instructions. Glutathione S-transferase protein expressed from the empty vector served as a negative control. Based on the study of VmE02 (Nie et al., 2019), we dissolved purified proteins in PBS buffer and diluted them to 500 nM for infiltrating *N. benthamiana* leaves. After 6 h of injecting purified TePDI or EV (empty vector) protein, the leaves were collected for ROS, callose, and defense-related genes detection.

Protein preparation and western blot analysis

Agroinfiltrated *N. benthamiana* leaves were collected at 24 hpi. Total plant proteins were extracted with a Plant Protein Extraction Kit (Solarbio, Beijing, China) following the manufacturer's instructions. Protein samples were loaded on a gel for SDS-PAGE (sodium dodecyl sulfate polyacrylamide gel electrophoresis). After electrophoresis, protein samples were transferred from the gel to a polyvinylidene difluoride membrane using the eBlot L1 Wet Protein Transfer System (GenScript, Piscataway, NJ, USA). Mouse anti-GFP

monoclonal antibody (Abmart, Shanghai, China) and goat anti-mouse IRDye 800CW (Odyssey, LI-COR) antibody were used as the primary and secondary antibodies, respectively. Protein bands were finally detected with an Odyssey imaging system (Li-COR) with excitation at 700 nm and 800 nm.

VIGS assays in *N. benthamiana*

VIGS was assayed using *A. tumefaciens* strains GV3101 harboring the pTRV1 vector and pTRV2:BAK1, pTRV2:SOBIR1, pTRV2:SGT1, pTRV2:HSP90, pTRV2:RAR1, pTRV2:NDR1, and pTRV2:EDS1 as described in a previous reference (Ma et al., 2015). The supernatant cells expressing TRV2 constructs were mixed with an *A. tumefaciens* culture expressing TRV1 in a 1:1 ratio in MES buffer (10-mM $MgCl_2$, 10-mM MES, 200-μM acetosyringone), to a final OD_{600} of 1.0. The mixed cell suspensions were then infiltrated into three primary leaves of four-leaf-stage *N. benthamiana* plants. The cell death phenotype was monitored at 3 dpi. pTRV2:PDS and pTRV2:GFP were used as positive and negative controls, respectively. The *N. benthamiana* leaves were collected to detect the silencing efficiency by RT–qPCR analysis. VIGS-related primers are listed in Supplemental Table S3.

RNA interference of *PDI* in spider mites and whiteflies

The RNAi-target regions of *TePDI* and *BtPDI* cDNA were amplified with primers containing the T7 promoter (20 bp; Supplemental Table S3). Red fluorescent protein was used as a control. Amplified products were purified with an AxyPrep DNA Gel Extraction Kit (Axygen, Union City, CA, USA) and then ligated to the pClone007 Vector (Tskingke). The constructed vector was sequenced to confirm the accuracy of amplified sequence before dsRNA synthesis. Then dsRNA was synthesized from PCR-generated DNA templates using a T7 High Yield RNA Transcription Kit (Vazyme).

TePDI in *T. evansi* was silenced as previously described with minor modifications (Xia et al., 2020). In brief, about 80 newly emerged female mites were soaked in dsRNA solution (800 ng/μL^{-1}) containing 0.1% Tween-20 (v/v) and incubated at 18°C for 24 h. Then the female mites were carefully transferred to tomato leaf discs (one untreated male mite was added to each leaf disc for mating). The number of female adults and laid eggs of dsRNA-treated spider mites were counted under a stereomicroscope 4 days later. The remaining live spider mites were used to measure RNAi efficiency. Approximately 25 mites were pooled as one biological replicate and each treatment contains three biological replicates.

To silence *BtPDI* in *B. tabaci*, newly emerged adult female whiteflies were fed on an artificial diet solution (15%, w/v, sucrose containing 500 ng/μL^{-1} dsRNA) for 2 days. Then, a female adult and a male adult were released on tomato leaves. Three days later, whitefly performance was assessed by counting the number of live adults and eggs laid on the leaves. RNAi efficiency was measured with remaining live whiteflies at that time.

Because spider mites and whiteflies are arrhenotokous, only the females were tested for dsRNA treatments. The efficiency with which the *T. evansi* and *B. tabaci* genes were silenced was validated by RT–qPCR as described above. The housekeeping genes *ATPase* and *rpl29* were used as the reference control for *T. evansi* and *B. tabaci*, respectively (Yang et al., 2015; Su et al., 2019). The primer sequences are listed in Supplemental Table S3.

To test plant defense responses to *TePDI*-silenced mites, one *N. benthamiana* leaf was divided into two sides along the main vein by insect glue. Half the leaf was infested with 30 ds*TePDI*-treated adults, while the other half was infested with 30 ds*RFP*-treated mites. The leaves were collected for defense response assays at 24 hpi. For tomato, different leaflets were infested with 15 ds*TePDI*-treated or ds*RFP*-treated *T. evansi* mites for 2 days, and were then collected for defense responses assays with the methods described above.

Choice preference assays

The feeding preference of *T. evansi* was determined with a two-choice test as previously described (Wei et al., 2014) with some modifications. Briefly, a rectangular-shaped bridge (length: 3 cm, width: 0.5 cm) made from Parafilm was positioned in the middle to connect leaf discs (20 mm Ø). The discs were put on a wet cotton-wool disk in a Petri dish (9 cm Ø). After 24 h of transiently expressing *GFP* or *TePDI* in *N. benthamiana*, these two types of leaves were made into leaf discs and placed at each end of the bridge. About 10–20 *T. evansi* females (2 ± 1 day old) were starved for 2 h and then simultaneously placed in the middle of the bridge. The numbers of spider mites on the two types of leaves were then recorded at fixed time intervals (2 h, 6 h, 12 h, 24 h, 36 h). These experiments were repeated eight times, each with 10–20 mites. Data were analyzed by χ^2 test and asterisks indicate a choice distribution significantly different from 50:50 ($\alpha = 0.05$). Similarly, after infiltration of purified 500-nM EV or TePDI protein into *N. benthamiana* for 6 h, leaves were used for choice preference assays as described above.

Spider mite survival assays on *N. benthamiana* leaves

The method of spider mite survival assays was conducted according to the previous study (Iida et al., 2019). *Nicotiana benthamiana* leaves were infiltrated with *A. tumefaciens* carrying TePDI and GFP for 24 h or were infiltrated by purified TePDI protein or EV solution for 6 h. Then the infiltrated leaves were made into leaf discs. Twenty adult female mites (2 ± 1 day old) were transferred onto a leaf disc (1 cm^2 each). Leaf discs were placed on the water-soaked cotton in the 10-cm Petri dish. Each dish contained eight discs. Survival of mites on the leaf discs was determined at 36 h after agroinfiltration or protein infiltration.

Phylogenetic analysis

Maximum likelihood (ML) trees were constructed with *PDI* CDS sequences. We searched PDI protein sequences with BALST-based search strategy using NCBI "nr" database. The

amino acid sequences were first aligned using MAFFT v7.407 (Katoh and Standley, 2013). Then, coding sequence alignments were generated with the guidance of MAFFT-generated amino acid alignments using PAL2NAL v14 (Suyama et al., 2006). The alignments were further edited using TrimAl v1.4.rev22 (automated1 mode; Capella-Gutiérrez et al., 2009) and then subjected to phylogenetic and selective pressure analysis.

To avoid situations of saturated substitution that results in poor phylogenetics, we assessed the substitution saturation of *PDI* CDS sequences using the substitution saturation test developed by Xia et al. (2003) with DAMBE v7.3.2 (Xia, 2018). No statistical evidence of substitution saturation was detected (Supplemental Table S6), meaning there is sufficient phylogenetic information in the PDI data set. We obtained the ML tree based on best-fit models calculated with ModelFinder (Kalyaanamoorthy et al., 2017), as implemented in IQ-TREE v1.6.10 (Nguyen et al., 2015). The PDI sequences from nonarthropod species were assigned as outgroups. The reliability of the phylogeny was evaluated with 1,000 ultrafast bootstraps.

Evolutionary rate analysis

To estimate the evolutionary rate of *PDI* coding genes, we employed the computer program codeml from the PAML suite v4.9j (Yang, 2007) and estimated the ω value (dN/dS) with the following models: one-ratio model (M0) and different site models (M1a, M2a, M7, M8, and M8a; Yang et al., 2000). To assess statistical significance, the null models (M0, M1, M7, M8a, and one-ratio model) were compared with alternative models (M2, M8, and free-ratio model) using the likelihood ratio test (LRT), which compares twice the difference in log-likelihood to a χ^2 distribution with degrees of freedom equal to the difference in model parameters. The LRTs were run with F3 × 4 codon frequency models, with an initial value of $\omega = 0.4$.

To determine evolutionary rates of *PDI* in comparison with other genes, we calculated the dN/dS value of genes that encode single-copy putative orthologs using codeml with the M0 mode in PAML. The single-copy putative orthologs were generated with OrthoFinder v2.5.4 (Emms and Kelly, 2015) from genomes of 15 arthropod species (Supplemental Table S7), whose food varies from plants to vertebrate blood. The longest protein isoforms of each gene were kept with a home-made bash script. For each single-copy ortholog group that was obtained for the PAML analysis, the codon-based alignment was generated with PAL2NAL (Suyama et al., 2006).

In situ hybridization

The DIG RNA Labeling Mix (Roche, Penzberg, Germany) and the T7 High Yield RNA Transcription Kit (Vazyme, Nanjing, China) were used to synthesize *TePDI* sense and antisense RNA probes. Primers for *TePDI* probes are listed in Supplemental Table S3. Hybridization was performed by *T. evansi* adults as previously described with some adjustment (Iida et al., 2019). Briefly, adult mites of *T. evansi* were washed with 50% NaClO (v/v) for 3 min and then by a 1: 1 mix of hexane and methanol for 3 min, followed by treatment with PBST (PBS containing 0.1% Triton (v/v)) for 10 min. Mites were prehybridized in a hybridization buffer for 1 h at 52°C. The probe was added to refreshed hybridization buffer and incubated overnight at 52°C. After hybridization, the mites were washed by a buffer (50% formamide (v/v), 2× SSC, and 0.1% tween-20 (v/v)) at 48°C for 25 min and then washed by PBSTB (PBS containing 0.1% Tween-20 (v/v) and 0.1% BSA (v/v)) at room temperature for 15 min. Then the mites were incubated with anti-digoxigenin-AP (1: 1,000; Fab fragments, Roche) in PBSTB at 4°C overnight. The mites were then washed with TBS buffer (100-mM Tris, pH 9.5, 100-mM NaCl, 0.1% Tween-20 (v/v)) for 15 min. TBST buffer containing FastRed substrate (Sigma-Aldrich, St Louis, MO, USA) was added to the mites and this was incubated in the dark at 4°C for 3 h. Methanol was then used to remove the background color and the mites were treated with 70% glycerol (v/v) in PBST (PBS containing 0.1% tween-20 (v/v)). Finally, the mites were sealed on slides and observed under a Leica confocal microscope.

Confocal microscopy

For subcellular localization, leaf discs of *N. benthamiana* were collected 24 h after *A. tumefaciens* treatment and were sent for confocal imaging on Zeiss LSM710 (Carl Zeiss, Oberkochen, Germany) with a 20× objective lens. GFP and mCherry fluorescence signal was observed at an excitation wavelength of 488 and 561 nm, respectively. The gains value is set between 600 V and 700 V. For *in situ* hybridization, FastRed fluorescence was visualized at an excitation wavelength of 633 nm using Leica TCS SP8 laser confocal microscope (Leica, Wetzlar, Germany) with a 20× objective lens. The gains value is set at about 566 V.

Statistical analysis

The data on plant defense genes expression and spider mite performance were compared between treatments by Student's *t* test. The spider mite choice assays were evaluated by a χ^2 test. For the expression pattern of *TePDI*, treatments were compared by one-way ANOVA followed by Tukey's post-hoc tests. All statistical analyses were conducted using the SPSS software package version 26.0 (SPSS Inc., Chicago, IL, USA).

Supplemental data

The following materials are available in the online version of this article.

Supplemental Figure S1. Screening of *T. evansi* elicitors.

Supplemental Figure S2. RNAi efficiency of *TePDI*.

Supplemental Figure S3. Phenotype of VIGS-treated *N. benthamiana* plants.

Supplemental Figure S4. Subcellular localization of TePDI and GFP.

Supplemental Figure S5. Similarity analysis of PDIs protein sequences in different organisms.

Supplemental Figure S6. Amino acid sequence alignment of TePDI across different species.

Supplemental Figure S7. Phylogenetic analysis of the *PDI* gene.

Supplemental Figure S8. PDI elicits the expression of key genes in defense-related pathways.

Supplemental Figure S9. BtPDI is required for whitefly performance.

Supplemental Table S1. Information for candidate salivary proteins.

Supplemental Table S2. Parameter estimates and LRT results for site models.

Supplemental Table S3. Primers used in this study.

Supplemental Table S4. Accession numbers of PDIs for phylogenetic analysis

Supplemental Table S5. Information for herbivores used in this study.

Supplemental Table S6. Substitution saturation test of PDI CDS with Xia index.

Supplemental Table S7. Genomes of arthropod species for ortholog analysis.

Acknowledgments

We are grateful to Dr Yan Wang, Dr Hai-Jian Huang, Dr Jing-Tao Sun, and Mr Yuan-Peng Xu of College of Plant Protection, Nanjing Agricultural University, China for their instruction and suggestions on the research. We are also thankful to Professor Jingwen Wang of School of Life Sciences, Fudan University, Shanghai, China for providing tick and mosquito cDNA samples.

Funding

The study was supported by the National Natural Science Foundation of China (32020103011, 32001905 and 31871976), the Natural Science Foundation of Jiangsu Province (BK20211213), and the Fundamental Research Funds for the Central Universities (No. KJQN202110).

Conflict of interest statement. None declared.

References

Alba JM, Schimmel BCJ, Glas JJ, Ataide LMS, Pappas ML, Villarroel CA, Schuurink RC, Sabelis MW, Kant MR (2015) Spider mites suppress tomato defenses downstream of jasmonate and salicylate independently of hormonal crosstalk. New Phytol **205**: 828–840

Armenteros JJA, Tsirigos KD, Sonderby CK, Petersen TN, Winther O, Brunak S, von Heijne G, Nielsen H (2019) SignalP 5.0 improves signal peptide predictions using deep neural networks. Nat Biotechnol **37**: 420–423

Bhattarai KK, Li Q, Liu Y, Dinesh-Kumar SP, Kaloshian I (2007) The *Mi*-1-mediated pest resistance requires Hsp90 and Sgt1. Plant Physiol **144**: 312–323

Bos JIB, Kanneganti TD, Young C, Cakir C, Huitema E, Win J, Armstrong MR, Birch PRJ, Kamoun S (2006) The C-terminal half of *Phytophthora infestans* RXLR effector AVR3a is sufficient to trigger R3a-mediated hypersensitivity and suppress INF1-induced cell death in *Nicotiana benthamiana*. Plant J **48**: 165–176

Bos JIB, Prince D, Pitino M, Maffei ME, Win J, Hogenhout SA (2010) A functional genomics approach identifies candidate effectors from the aphid species *Myzus persicae* (green peach aphid). PLoS Genet **6**: e1001216

Capella-Gutiérrez S, Silla-Martínez JM, Gabaldón T (2009) trimAl: a tool for automated alignment trimming in large-scale phylogenetic analyses. Bioinformatics **25**: 1972–1973

Chen ZQ, Wu Q, Tong C, Chen HY, Miao D, Qian X, Zhao XH, Jiang L, Tao XR (2021) Characterization of the roles of SGT1/RAR1, EDS1/NDR1, NPR1, and NRC/ADR1/NRG1 in *Sw-5b*-mediated resistance to tomato spotted wilt virus. Viruses **13**: 1447

Cui N, Lu H, Wang TZ, Zhang WH, Kang L, Cui F (2019) Armet, an aphid effector protein, induces pathogen resistance in plants by promoting the accumulation of salicylic acid. Phil Trans R Soc Lond B **374**: 20180314

Drurey C, Mathers TC, Prince DC, Wilson C, Caceres-Moreno C, Mugford ST, Hogenhout SA (2019) Chemosensory proteins in the CSP4 clade evolved as plant immunity suppressors before two suborders of plant-feeding hemipteran insects diverged. *bioRxiv*: 173278; DOI: 10.1101/173278

Du H, Xu HX, Wang F, Qian LX, Liu SS, Wang XW (2022) Armet from whitefly saliva acts as an effector to suppress plant defenses by targeting tobacco cystatin. New Phytol **234**: 1848–1862

Emms DM, Kelly S (2015) OrthoFinder: solving fundamental biases in whole genome comparisons dramatically improves orthogroup inference accuracy. Genome Biol **16**: 157

Erb M, Reymond P (2019) Molecular interactions between plants and insect herbivores. Annu Rev Plant Biol **70**: 527–557

Fan FG, Zhang Q, Zhang YN, Huang GZ, Liang XL, Wang CC, Wang L, Lu DP (2022) Two protein disulfide isomerase subgroups work synergistically in catalyzing oxidative protein folding. Plant Physiol **188**: 241–254

Fernández-Bautista N, Domínguez-Núñez J, Moreno MM, Berrocal-Lobo M (2016) Plant tissue trypan blue staining during phytopathogen infection. Bio-Protocol **6**: e2078

Fu JM, Shi Y, Wang L, Zhang H, Li J, Fang JC, Ji R (2021) Planthopper-secreted salivary disulfide isomerase activates immune responses in plants. Front Plant Sci **11**: 622513

Fu WC, Liu XZ, Rao C, Ji R, Bing XL, Li JB, Wang YY, Xu H (2021) Screening candidate effectors of the bean bug *Riptortus pedestris* by proteomic and transcriptomic analyses. Front Ecol Evol **9**: 760368

Gasteiger E, Gattiker A, Hoogland C, Ivanyi I, Appel RD, Bairoch A (2003) ExPASy: the proteomics server for in-depth protein knowledge and analysis. Nucleic Acids Res **31**: 3784–3788

Gouhier-Darimont C, Schmiesing A, Bonnet C, Lassueur S, Reymond P (2013) Signalling of *Arabidopsis thaliana* response to *Pieris brassicae* eggs shares similarities with PAMP-triggered immunity. J Exp Bot **64**: 665–674

Gross R, Zhang S, Wei LH, Caplan A, Kuhl J, Dandurand LM, Wang XF, Xiao FM (2020) The *Globodera pallida* effector GpPDI1 is a functional thioredoxin and triggers defense-related cell death independent of its enzymatic activity. Phytopathology **110**: 1838–1844

Guo HJ, Zhang YJ, Tong JH, Ge PP, Wang QY, Zhao ZH, Zhu-Salzman K, Hogenhout SA, Ge F, Sun YC (2020) An aphid-secreted salivary protease activates plant defense in phloem. Curr Biol **30**: 4826–4836

Hogenhout SA, Bos JIB (2011) Effector proteins that modulate plant-insect interactions. Curr Opin Plant Biol **14**: 422–428

Huang HJ, Cui JR, Chen L, Zhu YX, Hong XY (2019a) Identification of saliva proteins of spider mite *Tetranychus evansi* by transcriptome and LC-MS/MS analyses. J Proteomics **19**: e1800302

Huang HJ, Cui JR, Xia X, Chen J, Ye YX, Zhang CX, Hong XY (2019b) Salivary DNase II from *Laodelphax striatellus* acts as an effector that suppresses plant defence. New Phytol **224**: 860–874

Iida J, Desaki Y, Hata K, Uemura T, Yasuno A, Islam M, Maffei ME, Ozawa R, Nakajima T, Galis I, Arimura GI (2019) Tetranins: new putative spider mite elicitors of host plant defense. New Phytol **224**: 875–885

Ji R, Fu JM, Shi Y, Li J, Jing MF, Wang L, Yang SY, Tian T, Wang LH, Ju JF, et al. (2021) Vitellogenin from planthopper oral secretion acts as a novel effector to impair plant defenses. New Phytol **232**: 802–817

Jones JDG, Dangl JL (2006) The plant immune system. Nature **444**: 323–329

Jones JDG, Vance RE, Dangl JL (2016) Intracellular innate immune surveillance devices in plants and animals. Science **354**: aaf6395

Kalyaanamoorthy S, Minh BQ, Wong TKF, von Haeseler A, Jermiin LS (2017) ModelFinder: fast model selection for accurate phylogenetic estimates. Nat Methods **14**: 587–589

Kanneganti TD, Huitema E, Cakir C, Kamoun S (2006) Synergistic interactions of the plant cell death pathways induced by *Phytophthora infestans* Nep1-like protein PiNPP1.1 and INF1 elicitin. Mol Plant-Microbe Interact **19**: 854–863

Katoh K, Standley DM (2013) MAFFT multiple sequence alignment software version 7: improvements in performance and usability. Mol Biol Evol **30**: 772–780

Khan HA, Mutus B (2014) Protein disulfide isomerase a multifunctional protein with multiple physiological roles. Front Chem **2**: 70

Krogh A, Larsson B, von Heijne G, Sonnhammer ELL (2001) Predicting transmembrane protein topology with a hidden Markov model: application to complete genomes. J Mol Biol **305**: 567–580

Liao M, Hatta T, Umemiya R, Huang PL, Jia HL, Gong HY, Zhou JL, Nishikawa Y, Xuan XN, Fujisaki K (2007) Identification of three protein disulfide isomerase members from *Haemaphysalis longicornis* tick. Insect Biochem Mol Biol **37**: 641–654

Ma ZC, Song TQ, Zhu L, Ye WW, Wang Y, Shao YY, Dong SM, Zhang ZG, Dou DL, Zheng XB, et al. (2015) A *Phytophthora sojae* glycoside hydrolase 12 protein is a major virulence factor during soybean infection and is recognized as a PAMP. Plant Cell **27**: 2057–2072

Mattiacci L, Dicke M, Posthumus MA (1995) beta-Glucosidase: an elicitor of herbivore-induced plant odor that attracts host-searching parasitic wasps. Proc Natl Acad Sci USA **92**: 2036–2040

Mayor A, Martinon F, De Smedt T, Petrilli V, Tschopp J (2007) A crucial function of SGT1 and HSP90 in inflammasome activity links mammalian and plant innate immune responses. Nat Immunol **8**: 497–503

Meldau S, Baldwin IT, Wu J (2011) SGT1 regulates wounding- and herbivory-induced jasmonic acid accumulation and *Nicotiana attenuata*'s resistance to the specialist lepidopteran herbivore *Manduca sexta*. New Phytol **189**: 1143–1156

Meng YL, Zhang Q, Zhang MX, Gu B, Huang GY, Wang QH, Shan WX (2015) The protein disulfide isomerase 1 of *Phytophthora parasitica* (PpPDI1) is associated with the haustoria-like structures and contributes to plant infection. Front Plant Sci **6**: 632

Monaghan J, Zipfel C (2012) Plant pattern recognition receptor complexes at the plasma membrane. Curr Opin Plant Biol **15**: 349–357

Musser RO, Hum-Musser SM, Eichenseer H, Peiffer M, Ervin G, Murphy JB, Felton GW (2002) Herbivory: caterpillar saliva beats plant defences. Nature **416**: 599–600

Narindrasorasak S, Yao P, Sarkar B (2003) Protein disulfide isomerase, a multifunctional protein chaperone, shows copper-binding activity. Biochem Biophys Res Commun **311**: 405–414

Navajas M, de Moraes GJ, Auger P, Migeon A (2013) Review of the invasion of *Tetranychus evansi*: biology, colonization pathways, potential expansion and prospects for biological control. Exp Appl Acarol **59**: 43–65

Nguyen LT, Schmidt HA, von Haeseler A, Minh BQ (2015) IQ-TREE: a fast and effective stochastic algorithm for estimating maximum-likelihood phylogenies. Mol Biol Evol **32**: 268–274

Nie JJ, Yin ZY, Li ZP, Wu YX, Huang LL (2019) A small cysteine-rich protein from two kingdoms of microbes is recognized as a novel pathogen-associated molecular pattern. New Phytol **222**: 995–1011

Paulo JT, Godinho DP, Silva A, Branquinho C, Magalhaes S (2018) Suppression of plant defenses by herbivorous mites is not associated with adaptation to host plants. Int J Mol Sci **19**: 1783

Prince DC, Drurey C, Zipfel C, Hogenhout SA (2014) The leucine-rich repeat receptor-like kinase BRASSINOSTEROID INSENSITIVE1-ASSOCIATED KINASE1 and the cytochrome P450 PHYTOALEXIN DEFICIENT3 contribute to innate immunity to aphids in *Arabidopsis*. Plant Physiol **164**: 2207–2219

Rao WW, Zheng XH, Liu BF, Guo Q, Guo JP, Wu Y, Shangguan XX, Wang HY, Wu D, Wang ZZ, et al. (2019) Secretome analysis and *in planta* expression of salivary proteins identify candidate effectors from the brown planthopper *Nilaparvata lugens*. Mol Plant-Microbe Interact **32**: 227–239

Sarmento RA, Lemos F, Bleeker PM, Schuurink RC, Pallini A, Oliveira MGA, Lima ER, Kant M, Sabelis MW, Janssen A (2011) A herbivore that manipulates plant defence. Ecol Lett **14**: 229–236

Schimmel BCJ, Alba JM, Wybouw N, Glas JJ, Meijer TT, Schuurink RC, Kant MR (2018) Distinct signatures of host defense suppression by plant-feeding mites. Int J Mol Sci **19**: 3265

Schimmel BCJ, Ataide LMS, Chafi R, Villarroel CA, Alba JM, Schuurink RC, Kant MR (2017) Overcompensation of herbivore reproduction through hyper-suppression of plant defenses in response to competition. New Phytol **214**: 1688–1701

Schwessinger B, Ronald PC (2012) Plant innate immunity: perception of conserved microbial signatures. Annu Rev Plant Biol **63**: 451–482

Shangguan XX, Zhang J, Liu BF, Zhao Y, Wang HY, Wang ZZ, Guo JP, Rao WW, Jing SL, Guan W, et al. (2018) A mucin-like protein of planthopper is required for feeding and induces immunity response in plants. Plant Physiol **176**: 552–565

Shirasu K (2009) The HSP90-SGT1 chaperone complex for NLR immune sensors. Annu Rev Plant Biol **60**: 139–164

Snoeck S, Guayazán-Palacios N, Steinbrenner AD (2022) Molecular tug-of-war: plant immune recognition of herbivory. Plant Cell **34**: 1497–1513

Su Q, Peng ZK, Tong H, Xie W, Wang SL, Wu QJ, Zhang JM, Li CR, Zhang YJ (2019) A salivary ferritin in the whitefly suppresses plant defenses and facilitates host exploitation. J Exp Bot **70**: 3343–3355

Suyama M, Torrents D, Bork P (2006) PAL2NAL: robust conversion of protein sequence alignments into the corresponding codon alignments. Nucleic Acids Res **34**: W609–W612

van Bell AJE, Will T (2016) Functional evaluation of proteins in watery and gel saliva of aphids. Frontiers Plant Sci **7**: 1840

Villarroel CA, Jonckheere W, Alba JM, Glas JJ, Dermauw W, Haring MA, Van Leeuwen T, Schuurink RC, Kant MR (2016) Salivary proteins of spider mites suppress defenses in *Nicotiana benthamiana* and promote mite reproduction. Plant J **86**: 119–131

Wei JN, van Loon JJA, Gols R, Menzel TR, Li N, Kang L, Dicke M (2014) Reciprocal crosstalk between jasmonate and salicylate defence-signalling pathways modulates plant volatile emission and herbivore host-selection behaviour. J Exp Bot **65**: 3289–3298

Xia X, Peng CW, Cui JR, Jin PY, Yang K, Hong XY (2020) *Wolbachia* affects reproduction in the spider mite *Tetranychus truncatus* (Acari: Tetranychidae) by regulating chorion protein S38-like and Rop. Insect Mol Biol **30**: 18–29

Xia XH (2018) DAMBE7: new and improved tools for data analysis in molecular biology and evolution. Mol Biol Evol **35**: 1550–1552

Xia XH, Xie Z, Salemi M, Chen L, Wang Y (2003) An index of substitution saturation and its application. Mol Phylogenet Evol **26**: 1–7

Xu HX, Qian LX, Wang XW, Shao RX, Hong Y, Liu SS, Wang XW (2019) A salivary effector enables whitefly to feed on host plants by eliciting salicylic acid-signaling pathway. Proc Natl Acad Sci USA **116**: 490–495

Yang CX, Pan HP, Liu Y, Zhou XG (2015) Stably expressed housekeeping genes across developmental stages in the two-spotted spider mite, *Tetranychus urticae*. PLoS One **10**: e0120833

Yang ZH (2007) PAML 4: phylogenetic analysis by maximum likelihood. Mol Biol Evol **24**: 1586–1591

Yang ZH, Nielsen R, Goldman N, Pedersen AMK (2000) Codon-substitution models for heterogeneous selection pressure at amino acid sites. Genetics **155**: 431–449

Yuan MH, Jiang ZY, Bi GZ, Nomura K, Liu MH, Wang YP, Cai BY, Zhou JM, He SY, Xin XF (2021) Pattern-recognition receptors are required for NLR-mediated plant immunity. Nature **592**: 105–109

Zhao JL, Mejias J, Quentin M, Chen YP, Almeida-Engler J, Mao ZC, Sun QH, Liu Q, Xie BY, Jian H (2020) The root-knot nematode effector MiPDI1 targets a stress-associated protein (SAP) to establish disease in Solanaceae and *Arabidopsis*. New Phytol **228**: 1417–1430

Zhu YX, Song YL, Huang HJ, Zhao DS, Xia X, Yang K, Lu YJ, Hong XY (2018) Comparative analyses of salivary proteins from the facultative symbiont-infected and uninfected *Tetranychus truncatus*. Syst Appl Acarol **23**: 1027–1042